OFFSHORE SCALE MODEL WIND TURBINE

- OPERATION UNDER YAWED CONDITIONS -

Sarah Zecha
Jacob Bradshaw
Travis Hall

May 6, 2020

Contents

1. Acknowledgements

We would like to acknowledge our advisor Professor Martin Wosnik along with Jim Abare who helped us rewire the turbine and rewrite the LabView program that controls the wind turbine. We would also like to thank Scott Campbell for helping us with our motor issues. Additional thanks to Professor Alireza Ebadi and Chase Klewicki for their continued support in the FPF.

2. Abstract

Wind turbines are typically placed in regularly spaced arrays. One major issue for arrays is wake loss, which causes the overall power output of a wind farm to drop. One potential solution to this problem is known as wake steering. Wake steering yaws some turbines with the intention of deflecting the wake away from downstream turbines, thereby decreasing the power in the upstream turbines in an array which lowers the power output of a few turbines to increase the power output of the wind farm overall. Preliminary analysis with a 1 meter HAWT scale wind turbine is performed with the intention for further analysis and experimentation. Setting up the turbine required a new understanding of DAQ board wiring and LabView setup and analysis, as well as instrumentation set up. A theoretical power curve is constructed using Qblade, and the turbulent-boundary-layer spire requirements for the UNH FPF are calculated. The hope for this project is full preparation for atmospheric boundary layer simulation and wind turbine experiments in ideal and yawed conditions in the future. Experiments with the 1m research turbine under non-yawed and yawed operating conditions were planned, but due to COVID-19 shutdown the project pivoted to tasks that could be completed while working remotely.

3. Introduction

Wind energy is one of the fastest growing sources of renewable energies in the United States. Currently, the majority of electrical energy produced in the US is from nonrenewable energy sources which is leading to an accelerated effect of greenhouse gas emissions [7]. In order for renewable energy sources to become the primary means of energy, more research needs to be conducted. Wind turbines are being used throughout the country and across the globe in both onshore and offshore wind farms. Due to the unpredictability of wind currents, engineers are continuously tasked with finding methods to improve performance of the turbines and increase the net power output of wind farms.

The wind energy industry first started in 1887 when the first wind turbine was constructed to produce electricity [11]. Consisting of 144 rotor blades while spanning a diameter of 17m, this vintage turbine produced nearly 12kW of electrical energy [11]. Fast forward a few decades, and the advancement of wind technology spread throughout the United States and in Denmark. By 1941 in Castleton, Vermont, the first megawatt turbine was installed and connected to a local power grid for distribution [11]. In just over 50 years (1887-1941), wind technology increased power output by nearly 100 times and moved from providing for individuals to more large scale projects.

By the late 1970's, engineers developed the idea of implementing wind turbines placed in arrays to capture mass amounts of power in a single valley. At first, these arrays of wind farms were designed with a generating capacity of around 600 kW, but over the past decade, they have obtained much higher capacities reaching up to 20,000 MW in the Gansu Wind Farm in China [2]. These massive arrays however, come at a large cost and can span thousands of acres in order to achieve generating capacities as high as Gansu.

Scaled models have been an essential tool for engineers to further study the dynamic interaction between the wind current and the turbine. Large wind farms with typical spacing create blockage and wake losses, which means without the use of wake steering, arrays are forced to consume large sections of open fields both onshore and offshore. The challenge engineers are now facing is how to more effectively reduce wake losses by implementing wake steering where the changing of yaw angles is used to increase power available in the wind downstream.

The scope of research discussed in this paper intends to understand the basic specs of the 1m model horizontal axis wind turbine (HAWT) and the effects of wind speed on power output. Power curves will be created for different wind speeds and for different yaw angles with both uniform inflow conditions and turbulent boundary layer inflow conditions. Additionally, the paper will investigate the importance of wake steering on power generation efficiency in wind farm arrays. Future plans for experimentation with comparing the performance of the 1m HAWT under non-yawed and yaw conditions along with wake steering will also be discussed in detail.

4. Motivation

4.1 Industry

As the need for renewable energy sources increases in the world, so does the need for research models that validate the designs of those renewable energy sources. In this case, the testing and validation of wind turbines helps those who design wind farms and turbine arrays to optimize their design. Wind is a renewable resource that is highly variable and intermittent. The best wind resource is found higher up in the Earth's boundary layer because that is where the wind is faster and there are less obstacles in the way. In order to best take advantage of the resource available, whether onshore or offshore, more than one wind turbine needs to be installed where there is a good resource. These turbines are most often arranged in a grid pattern, however a grid pattern is not the most productive formation for an array of turbines. This is because if the wind is perpendicular to the turbines, the first row operates at maximum production for that wind speed but the second row and every row after will receive less and less wind which decreases their production and efficiency.

The importance of studying wind turbines and figuring out how to optimize their performance is demonstrated by the rapid growth the wind energy industry has seen in the past 30 years. As shown in Figure 4.1 below, there was almost no wind energy electricity generation in 1990 and that increased to over 300 billion kWh in 2019 [17].

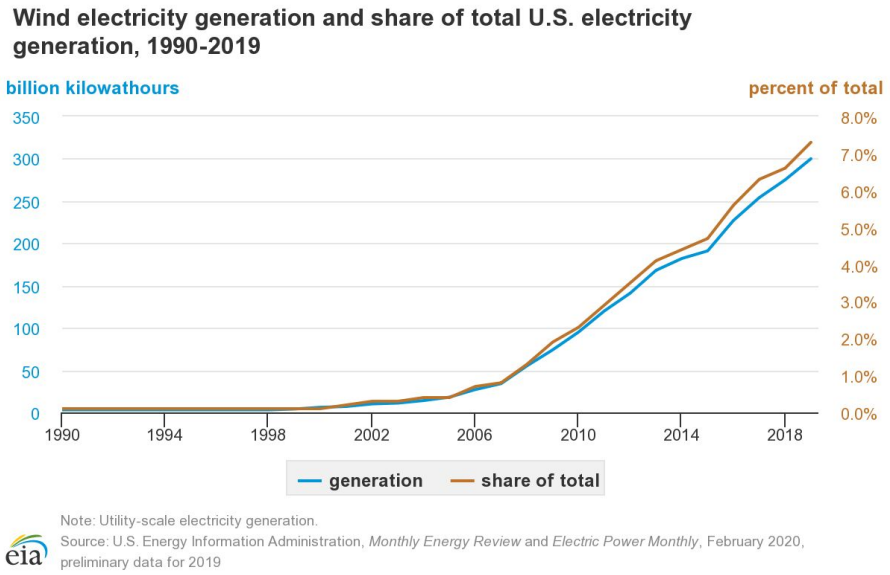

Figure 4.1 - EIA graph of wind energy electricity generation from 1990-2019 [17].

With the increase in generation comes an increase in wind energy companies, farms, and problems. Those increases are the reason for the research being done in the University of New

Hampshire (UNH) Flow Physics Facility (FPF). By creating accurate experimental models, the research will help grow the wind energy field even more.

4.2 Wake Steering

To maximize the overall performance of a wind farm, researchers are exploring something called wake steering. Wake steering is when turbines in an array are turned, or yawed, to one side or the other in order to maximize the amount of flow the turbines downstream of the yawed turbines are receiving. If done correctly, this will maximize the power output and the performance of the wind farm as a whole. There are several ways to study the performance of wind turbines and simulate their performance and wakes under yaw. Some of the ways to study wake steering are through the use of full-scale wind turbines, SWiFT-scale turbines, and as-large-as-feasible turbines in large wind tunnels [13]. The 1m model HAWT used for testing at UNH is of the last variety. The problem with testing using full-scale wind turbines, and even SWiFT-scale turbines is that it is practically impossible to control the inflow that these turbines are receiving which means that it is hard to accurately control and reproduce experimentation. However, wake steering experimentation has been conducted at the SWiFT facility in Texas. At this facility, which was commissioned by the Department of Energy in 2013 and is run by Sandia, there is a wake imaging system which is designed to measure the "formation and development of flow structures near the turbine rotor" in 3D [13]. In a paper published by NREL and Envision Energy in 2017, a team of researchers used the Longyaun Rundong Chaojiandai offshore wind farm in Jiangsu, China to test the results of yaw controlled wake steering on the combined performance of multiple wind turbines. The turbines used were Envision EN136/4 MW turbines. Of the 25 turbines in the farm, only five were used in the experiment. One was a control turbine (C1), three were the turbines in the wake (D1, D2, D3) which were 7 diameters and 340^{o} away, 8.4 diameters and 51^{o} away, and 14.3 diameters and 81^{o} away. The fifth turbine was a reference turbine outside of the influence of the other turbines (R1) [5]. The setup can be seen in Figure 4.2 below.

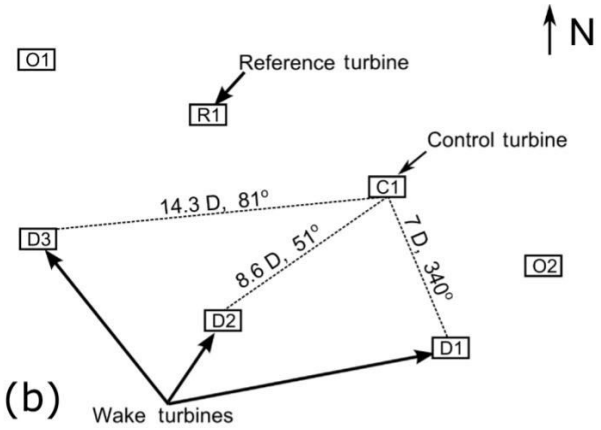

Figure 4.2 - Offshore wind farm experimental setup [5].

They found that the overall performance of the collective turbines did improve when the wakes were controlled by yaw and steered away from the turbines downstream of the controlled turbine [5]. The best results were found with the turbines that were 7 diameters and 8.4 diameters away. These results have been confirmed by testing done at the SWiFT site [13]. However, both of these tests were not conducted in a facility as controlled as the FPF at UNH. By conducting more performance and yaw control experiments, the research at UNH could further validate the results found during field testing. Through validating that yaw-controlled wake steering is a way to increase overall power output at a wind farm, wind farm operation could change and the amount of energy generated from wind energy globally could increase.

4.3 Importance of the Research

As mentioned in the previous section, the knowledge of harnessing wind energy has been rapidly increasing since the early 2000's. More countries have been investing an ample amount of resources to understand how to more effectively integrate wind turbines into their renewable power generation scheme. However, because it is extremely difficult to predict wind currents, some countries resort to other cost effective alternatives or entirely resist from renewable energy in general. That is why it is vital to the industry to understand how to maximize the energy that can be extracted from the wind when the source is at prime condition. This is where the need for extensive testing and performance analyses surface.

In terms of testing, it is not practical to test a full-scale wind turbine simply because of how expensive the structures are along with the cost of installation. To gage quality tests would be near impossible due to the amount of uncontrolled variables such as having a controlled steady wind profile and speed. Additionally, numerical flow simulations for large scale wind farms can be insufficient because of the computing power needed to obtain necessary measurements for optimizing blade design and array mapping. For these reasons, it is imperative that scaled down experiments be run in a controlled wind tunnel environment. This is what the UNH 1m HAWT plans to be utilized for in the FPF (Flow Physics Facility).

The 1m scale research turbine is based on the NREL 5MW reference turbine scaled to a ratio of 1:126 [3]. This scaling was sized in correlation with the testing facility and was designed to be large enough where Reynolds Number independent performance curves could be obtained, while having reasonable blockage (<5%) [3]. Moreover, the size of the model research turbine is ideal for collecting sufficient data on the wake interaction with the turbulent boundary layer. This type of data can be used to gain insight into wake behavior and validate potential numerical models developed on the larger grade. Research in these areas is critical for the advancement of the wind industry. Such data can further increase efficiency of currently installed turbine arrays and better prepare for future installments.

Furthermore, a secondary benefit of the research is potential for educational purposes at the university's undergraduate level. Improvements and extensions of this project will introduce

the complexities of the work to many student groups in the years to come. Much more can be done with this 1m model turbine. There is an ideal configuration for yaw control for a given array of wind turbines, and one day this project may lead to insight on what that may be.

5. Background

5.1 Power Performance Theory

The 1m model Horizontal Axis Wind Turbine (HAWT) used in this study is modeled after the NREL 5MW research wind turbine. NREL's 5MW research wind turbine has a diameter of 126 meter so based on that, the model turbine used for this study has a 1:126 scale [3]. The facility used to test the model turbine is the Flow Physics Facility (FPF) at the University of New Hampshire in Durham, New Hampshire. The test section in the FPF is 72 meters long, 6 meters wide, and 2.7 meters tall [3]. The model turbine was designed with these parameters in mind, and when it is being tested in the front of the test section, the center of the nose on the nacelle sits at 1.35 meters tall which is exactly in the center of the tunnel. When running, the turbine blocks about 4.85% of the test section which was chosen on purpose so that the power and thrust would not be significantly affected [3].

In order to appropriately measure and quantify the performance of the 1m model HAWT, information needs to be gathered about the power available in the wind, the wind speed, and the rotation of the turbine. The power available in the wind can be described as,

$$P_{available} = \tfrac{1}{2}\rho A U^3 \tag{5.1}$$

Where ρ is the density of the air based on the temperature of the testing conditions, A is the area covered by the rotor, and U is the velocity of the wind (usually measured by pitot tube). The power taken from the wind by the wind turbine can be derived from 1-D momentum theory as:

$$P = \tfrac{1}{2}\,\rho\, A\, U_1{}^3\; 4a(1-a)^2 \tag{5.2}$$

Where a is the axial induction factor. The axial induction factor is the fractional decrease in velocity at the rotor and can be described by the below equation:

$$a = \frac{U_1 - U_2}{U_1} \tag{5.3}$$

The coefficient of power is another tool used to describe the performance of the wind turbine in a non-dimensional way that enables comparison between turbines. The coefficient of performance can be described as:

$$C_p = \frac{P}{\tfrac{1}{2}\rho\, A\, U^3} \tag{5.4}$$

Where P is the power from the wind turbine and the denominator is the power available in the wind. The coefficient of power can also be described with the following equation:

$$C_p = 4a(1-a)^2 \tag{5.5}$$

Which just uses the axial induction factor to describe the performance of the turbine. Using equation 5.3 and equation 5.5 and the derivative of the C_p equation with respect to a, the theoretical limit to power production can be found as:

$$C_{p,max} = \frac{16}{27} = 0.593 \tag{5.6}$$

when the derivative is equal to zero. This is also referred to as the Betz limit. It means that all wind turbines can theoretically only be 59.3% efficient. So far, that hasn't been disproven by wind turbines in use which can achieve about 50% efficiency. The other parameter used to measure wind turbine performance is the tip speed ratio. The tip speed ratio is the ratio between the tip speed of the rotor (ΩR) and the velocity of the wind (U). The tip speed ratio uses the following equation:

$$\lambda = \lambda_r \frac{R}{r} = \frac{\Omega R}{U} \tag{5.7}$$

Where λ_r is the local tip speed ratio, R is the total radius of the rotor, r is the local radius, Ω is the angular velocity, and U is the wind speed.

Another wind turbine performance parameter is thrust. Thrust is calculated using similar parameters to power calculations. To calculate thrust force directly, the following equation is used:

$$T = \frac{1}{2}\rho A U^2[4a(1-a)] \tag{5.8}$$

Where the variables have the same meanings as above equations. Using that equation, the coefficient of thrust can also be calculated using the following equation:

$$C_T = \frac{T}{\frac{1}{2}\rho U^2 A} = 4a(1-a) \tag{5.9}$$

This equation shows that the thrust coefficient is essentially the ratio between the thrust force and the dynamic force and can be simplified down so that it is just described by the axial induction factor.

5.2 Calibration

5.2.1 Load Cell Calibration

The load cell that measures thrust on the wind turbine was calibrated for two different load cases. The first case of loading is when a flow is introduced onto only the tower while the second case of loading is when the whole turbine is in the flow. For the tower only case, the

calibration weights were applied at 0.59 meters from the base of the tower. To ensure the force balance rails were supporting the same load they would be during tower only testing, the turbine nacelle was removed during this calibration. For the full turbine case, the loading was applied at a height of 1.30 meters from the base. A schematic of the two calibration load cases is provided in Figure 5.1.

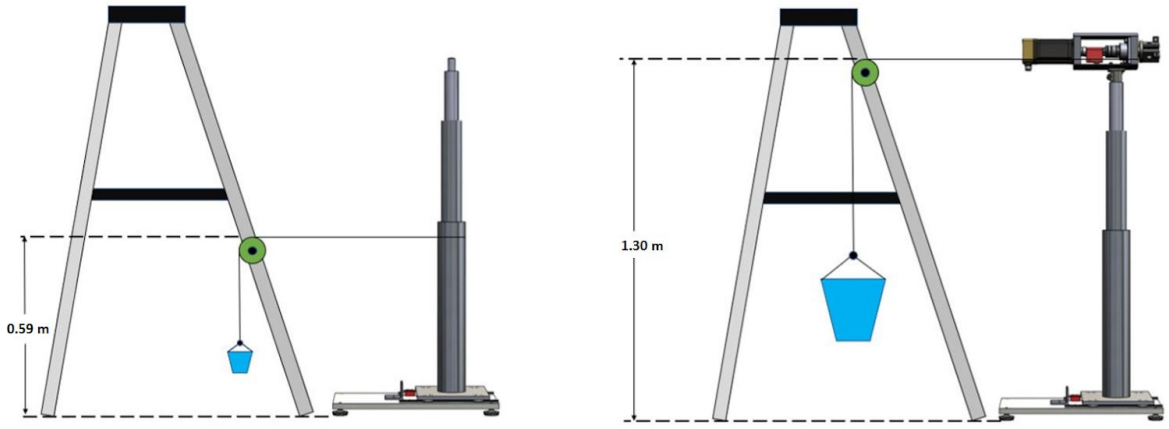

Figure 5.1 - A schematic outlining the force balance calibration for two load cases. Tower only testing and full turbine loading are on the left and right side respectively [3].

The calibration weights were added incrementally from 9.81 N to 77.9 N for both the full turbine and the lower tower cases. Loading and unloading techniques were used to better gage the sensitivity of the load cell. These results for the calibration curves are provided below in Figures 5.2 and 5.3.

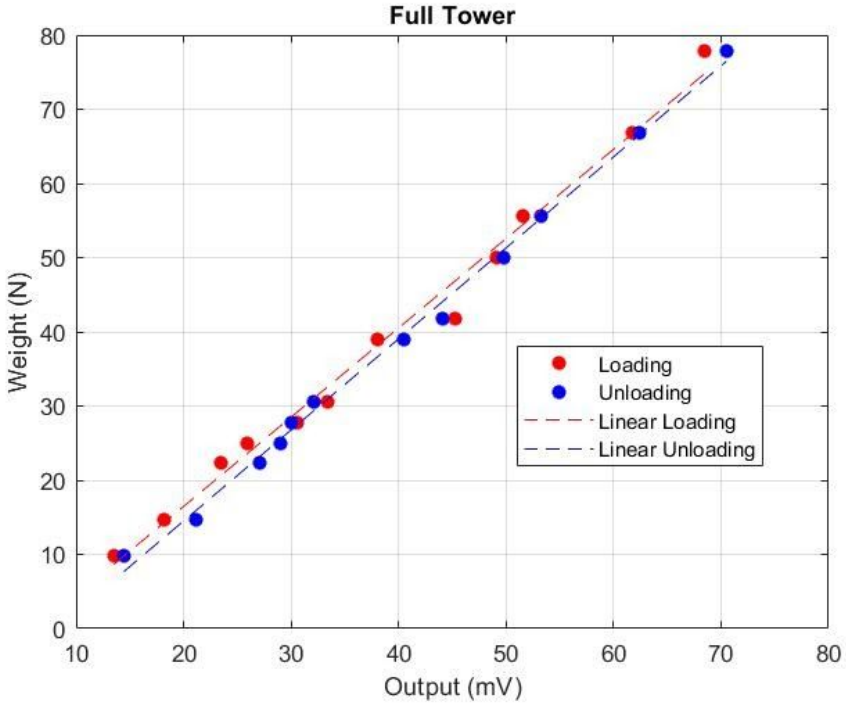

Figure 5.2 - Calibration curve for the complete turbine build. The curve was constructed by loading and unloading the force balance at a location 0.59 m from the ground surface.

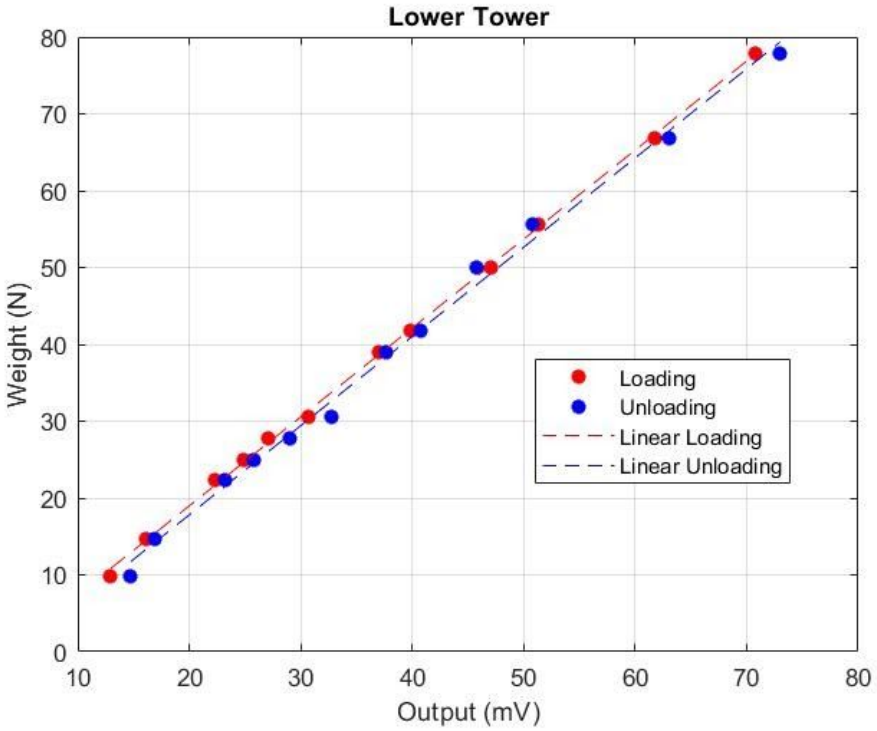

Figure 5.3 - Calibration curve for the lower tower build. The curve was constructed by loading and unloading the force balance at a location of 1.30 m from the ground surface.

The load cell used in the force balance is accurate to ± 0.111N. The hysteresis that is seen in Figure 5.2 is larger than this uncertainty proving that there is some stiction in the ball bearing carriages on the force balance. To quantify the stiction in the bearings, the top plate of the force balance was slid forward, out of contact with the load cell, and weights were added until movement of the force balance occurred. The stiction in the bearings was determined to be about 4.7 N.

5.2.2 Torque Calibration

Power is lost during turbine operation to the bearings in the motor. The power that is lost is dependent on the rotational rate of the turbine. To quantify the power lost, a bearing torque calibration was performed. The blades were removed from the turbine before calibration to ensure more accurate results. The turbine was spun at a range of rotational velocities from 700 RPM to 1400 RPM which correlate with the range of expected rotational speeds for performance testing. The torque at each of the speeds was quantified using a TRS605 rotational torque transducer. A calibration curve relating the rotational velocity of the turbine to the power lost to the bearings was generated and is shown in Figure 5.4. It should be noted that the TRS605 rotational torque transducer is accurate to ±0.01 Nm and the torque from the bearings was on the order of 0.03 Nm [3]. The power lost to the bearings was determined to range from 2.1W to 4.5W depending on rotational velocity.

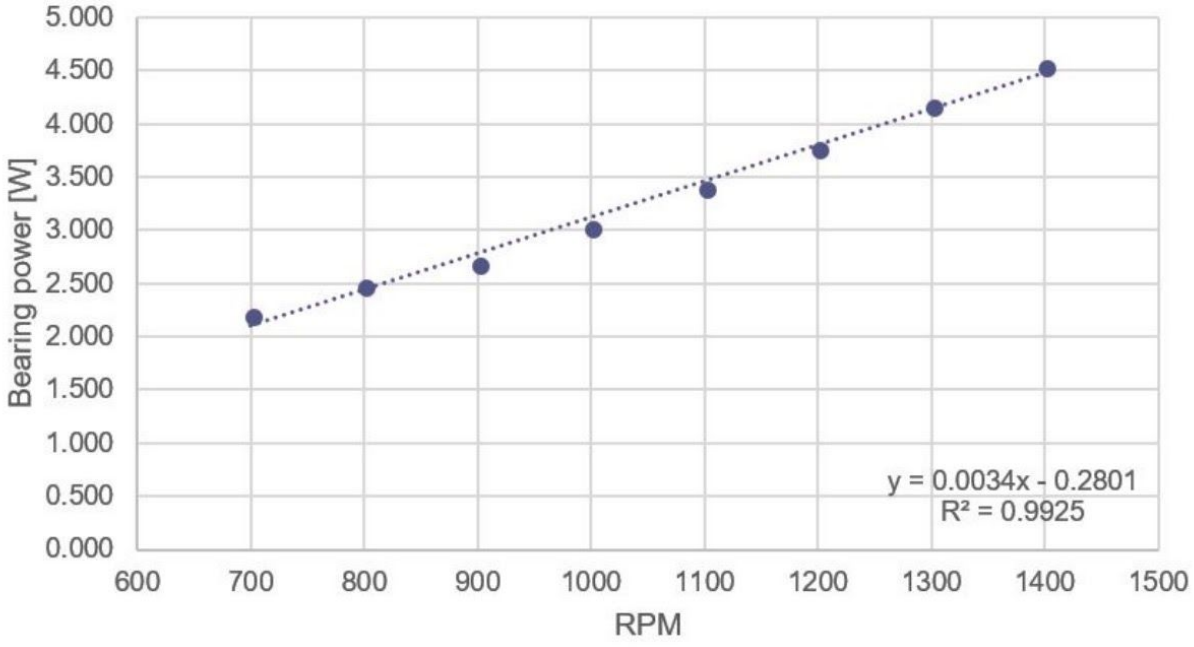

Figure 5.4 - Calibration curve for the power lost to the bearings during rotational rates ranging from 700 to 1400 RPM [3].

5.3 Varying Blade Pitch Angle

The pitch of the blades can be set and adjusted manually using a laser alignment jig that attaches to the blade. The laser jig is placed on the tip of the blade at 7.875 inches from the tip. A laser line is projected onto the wall that is parallel to the blade. This line is denoted by the 'Makita laser line' as seen in Figure 5.5. A secondary laser is fastened to the alignment jig and projected onto the same wall which is denoted as the 'Calpac Alignment Laser (line)' in the same figure as previously mentioned. Using the geometric relationship between the two lasers and the known distance of projection, the blade pitch angle can be properly controlled with a confidence within ±0.25 degrees [3]. The procedure for adjusting the pitch angle is listed below. See Figure 5.6 for a description of the pitch control assembly.

1. Loosen the holding screw.
2. Toggle with adjustment screw to control the laser dot to the desired pitch location. Note that each full rotation of the adjustment screw equates to 0.57 degrees of pitch.
3. Lock the adjustment screw.
4. Tighten the holding screw and take measurements.
5. Repeat steps 1 through 4 for the other two blades for each pitch angle adjustment.

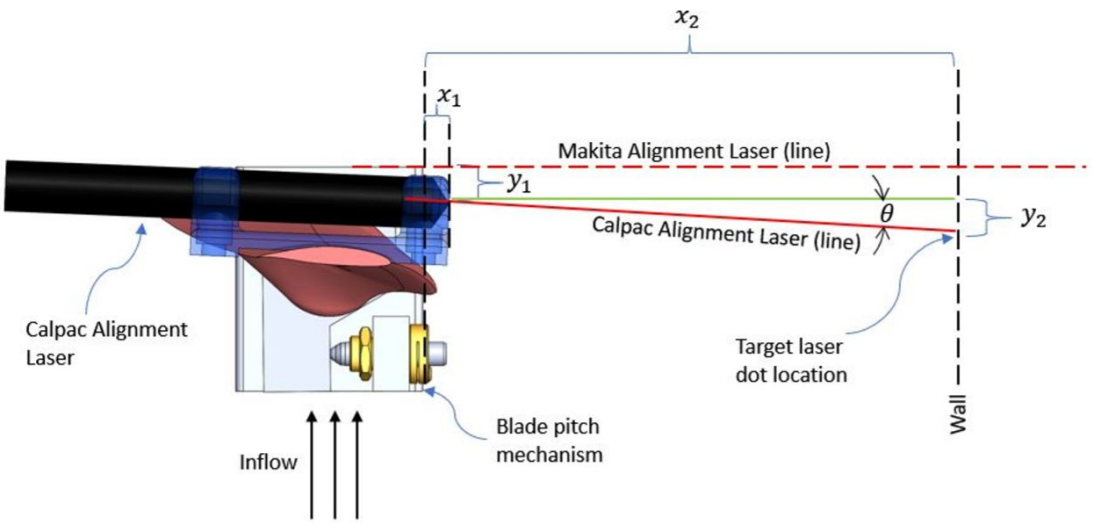

Figure 5.5 - Laser alignment schematic for adjusting blade pitch angle [3].

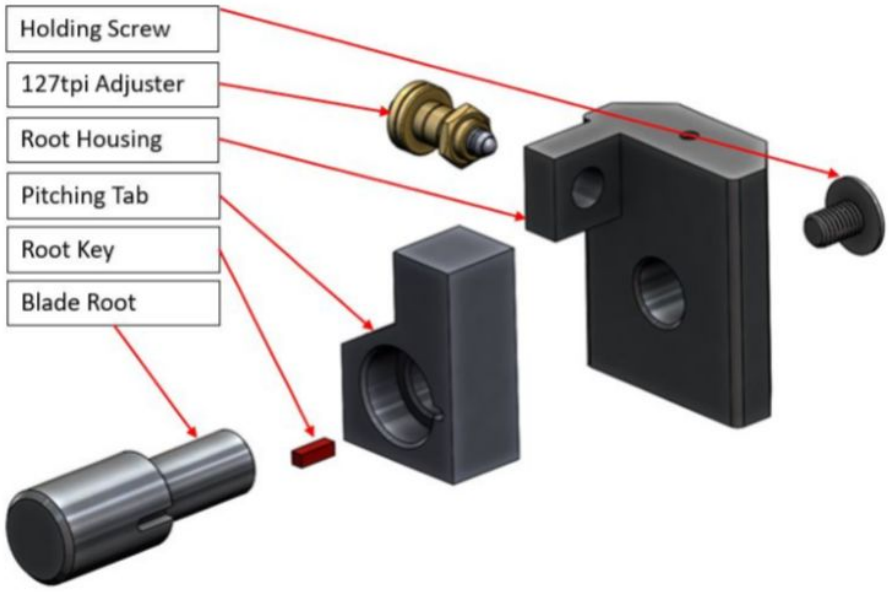

Figure 5.6 - Pitch control assembly for the laser alignment jig [3].

In a similar manner, the yaw angle can be controlled by affixing one laser to the turbine and one laser to the base of the turbine. From there, the angle between the two lasers can be measured using a geometric relationship with the known distances. Controlling both the yaw angle of the turbine and the blade pitch angle are necessary for understanding the performance of the turbine. Yaw angle studies have further research possibilities which apply to turbine array formations and wake steering to overcome power reduction in the wind downstream from the initial turbine.

5.4 Inflow Mapping

To initialize testing, an inflow map was created using pitot tubes positioned 5m from the entrance of the wind tunnel. This location was chosen specifically because the model turbine would be placed at 8m from the entrance for the uniform flow simulation so ensuring a uniform flow was necessary for testing. Under the assumption that the flow is symmetrical about the vertical axis in the center of the rotor of the turbine, only half of the wind tunnel flow was measured to create a more efficient testing process. To show a full inflow map, the flow field from the measured data was used to replicate the other half of the flow.

Measurements were taken at the center of the rotor and at the middle and tip of each blade in the horizontal and vertical directions. Measurements were also taken at one point beyond the blade in both the positive and negative y-directions and halfway between the wall. The wind speed was measured halfway between the end of the blade and at the wall, and at the wall in the x-direction as well. From this collection of points, a full grid of 35 points were

developed and the inflow of the FPF was mapped as seen in Figure 5.7. To verify the assumption of symmetry, three measurements were taken on the other side of the turbine which are represented by marked “x’s” below.

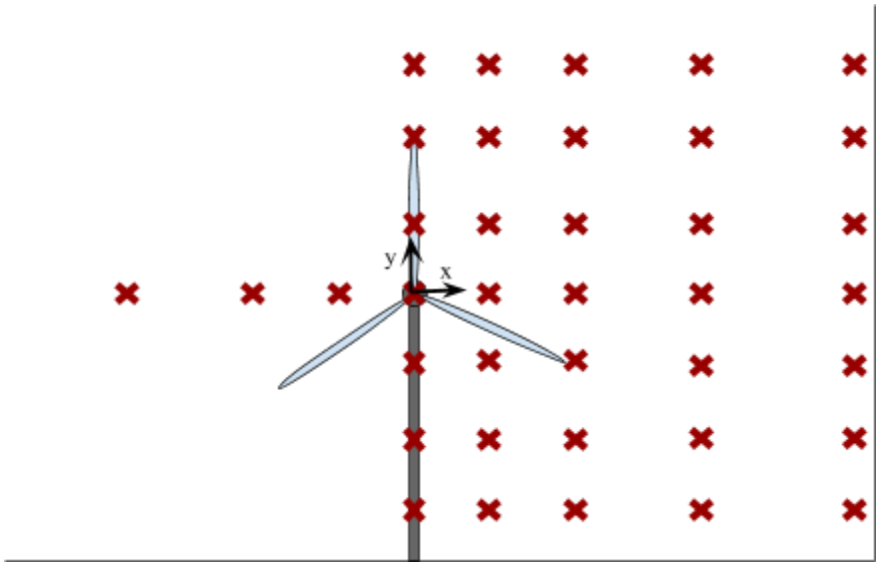

Figure 5.7 - Diagram of the grid points used to map the inflow of the wind tunnel. The two sides of the wind tunnel are considered to be symmetrical.

The measurements were collected with a pitot tube and then converted using a pressure transducer. While testing, the pitot tube collected data at each point for one minute to gather a sufficient amount of data to reduce noise. However, at the center of the rotor, the pitot tube collected data for 20 minutes to analyze the stability and turbulence intensity of the incoming flow. The flow at 5m downstream from the inlet did prove to be uniform and can be seen in Figure 5.8. Before testing occurs for the offshore simulated condition, another inflow map will need to be created. This will ensure that the boundary layer created is what is needed to fully encapsulate the turbine and be certain there is no interference from the ceiling boundary layer where the turbine is located.

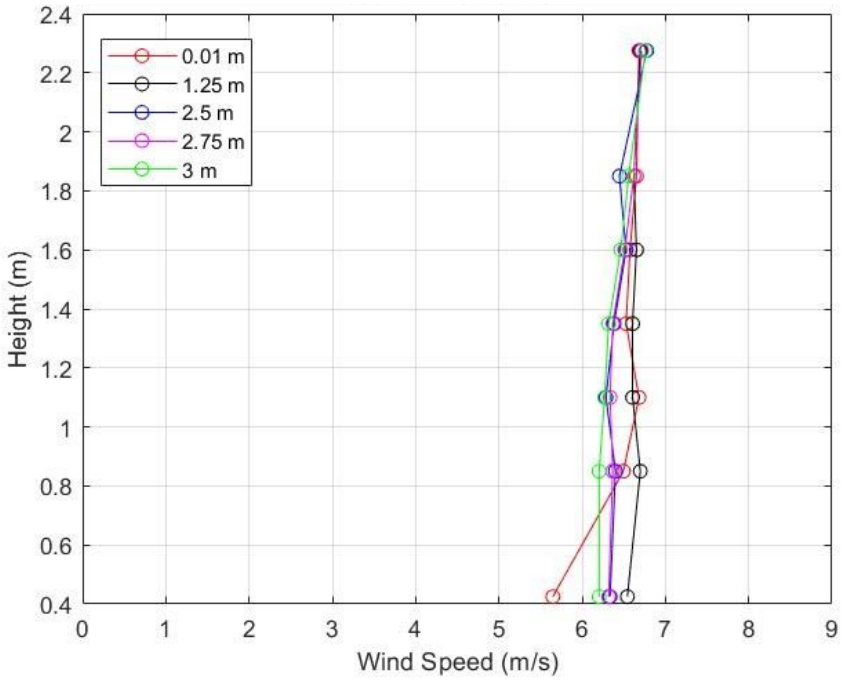

Figure 5.8 - Side view of the flow profile in front of the turbine for fan speed of 600 RPM. Each line represents the distance from the side wall where the red curve is at the wall and the green curve is in the center of the tunnel.

5.5 Uncertainty Analysis

Each instrument used to determine the velocity of the wind has some error associated with it. To find uncertainty for the wind velocity measurement, which is used to control the turbine RPM speed, a taylor series expansion for propagation of uncertainty is used [15]. The measurements that primarily contribute to this uncertainty are the temperature and pressure measurements.

$$\text{Uncertainty}_{\text{Uinf}} = \sqrt{\left(\frac{dU_\infty}{dP}\right)^2 (u_P)^2 + \left(\frac{dU_\infty}{dP_{atm}}\right)^2 (u_{P_{atm}})^2 + \left(\frac{dU_\infty}{dT}\right)^2 (u_T)^2} \qquad (5.8)$$

Here U_∞ is the computed velocity, P is pressure difference from the pressure transducer, and T is temperature from a thermocouple. u_p and u_T are the individual uncertainties from each measurement and are listed below.

Table 5.1 - Measurement uncertainty from Taylor-Power Masters Thesis [14].

Measurement	Source	u
Pressure	Pressure Transducer	±0.15%
Pressure	Digitization	±0.0015 torr
Temperature	Thermocouple Stability	±0.025 °C
Temperature	Thermocouple Gain	±0.25%
Temperature	Digitization	±0.15°C
Atmospheric Pressure	Barometric Shift	±0.0375 torr

To find uncertainty, first write the equation for wind velocity.

$$U_\infty = \sqrt{\frac{2PRT}{P_{atm}}} \tag{5.9}$$

Re-writing this equation into the uncertainty equation gives,

$$u_{U_\infty} = \frac{1}{2} U_\infty \sqrt{\left(\frac{u_P}{P}\right)^2 + \left(\frac{u_{P_{atm}}}{P_{atm}}\right)^2 + \left(\frac{u_T}{T}\right)^2} \tag{5.10}$$

Without having run live tests, the best estimate of uncertainty would be from using data from the Taylor-Power thesis. Using the equation and the values above, the total relative uncertainty of the wind in the thesis, on average, was $U_{U\infty}/U_\infty$ = 1.63 % [14].

6. Turbine Wiring

Wiring the turbine was an unexpected challenge that took a large portion of project time to finish. The scope of the project changed when the scale wind turbine testing system was found to be missing the brains of the operation. The DAQ board that channeled all inputs and outputs of the system was removed from the setup. This problem was exacerbated by the lack of documentation concerning the wiring of the DAQ. A new DAQ was purchased but very few clues were given as to where each device was to be wired. At this point the team worked to understand each subsystem of the turbine and how they all fit together, while learning LabView and a little bit about the safety hazards involved in electrical work. Most of the major breakthroughs came from the help of Jim Abare, a TSC Electronics Engineer at the University of New Hampshire. Jim's knowledge of LabView and electric systems was immeasurably helpful. He was able to educate the team and work out the kinks in the system that was nearly running. With his help, the turbine was up and running shortly after the new year (in 2020).

The system is made up of a few components. The most major being the model turbine itself. The turbine needed power, however, and also a reference wind speed to be set to a desired tip speed ratio. Power is supplied by a 240 watt outlet in the FPF storage hall. Wind speed is determined using temperature and pressure, with a thermocouple and pressure transducer pitot tube system respectively. A torque cell was used to read the RPM of the rotor while a load cell was used to analyze the thrust on the tower. Ideally all of these systems would be connected to the DAQ and controlled with a LabView program. The system that was tested initially took temperature values inputted manually, under the assumption that the changing temperature throughout a single test would not vary greatly enough to affect the result. However, a persisting issue with the data collection from the pressure transducer led the team to switch to a manual input for this variable as well.

Presented in Figure 6.1 below is the complete layout for the hardware used to control the 1m HAWT. In order to drive the turbine blades, power must be run from the central 240 W outlet to the Compax3 device which is used to control the servo motor positioned in the nacelle. The power supply is labeled in the figure and is operated manually with an on-off switch. When the power supply is turned out, a green LED should light up on the Compax3 and hold steady, representing a stable connection. Note that a slow flashing light means that the axis is without excitation and therefore no power is being supplied to the motor [10]. As labeled in the figure, the two yellow lines are where the power is transferred from the Compax3 to the servo motor. Due to the fact that the Compax3 has a large amount of current running through the device, a resistor bank, which is set up on the left side of the cart, is used to maintain the appropriate amount of resistance in the circuit. With changing rotor speeds, it is important to have a resistor bank that changes resistance with various loads and motor speeds.

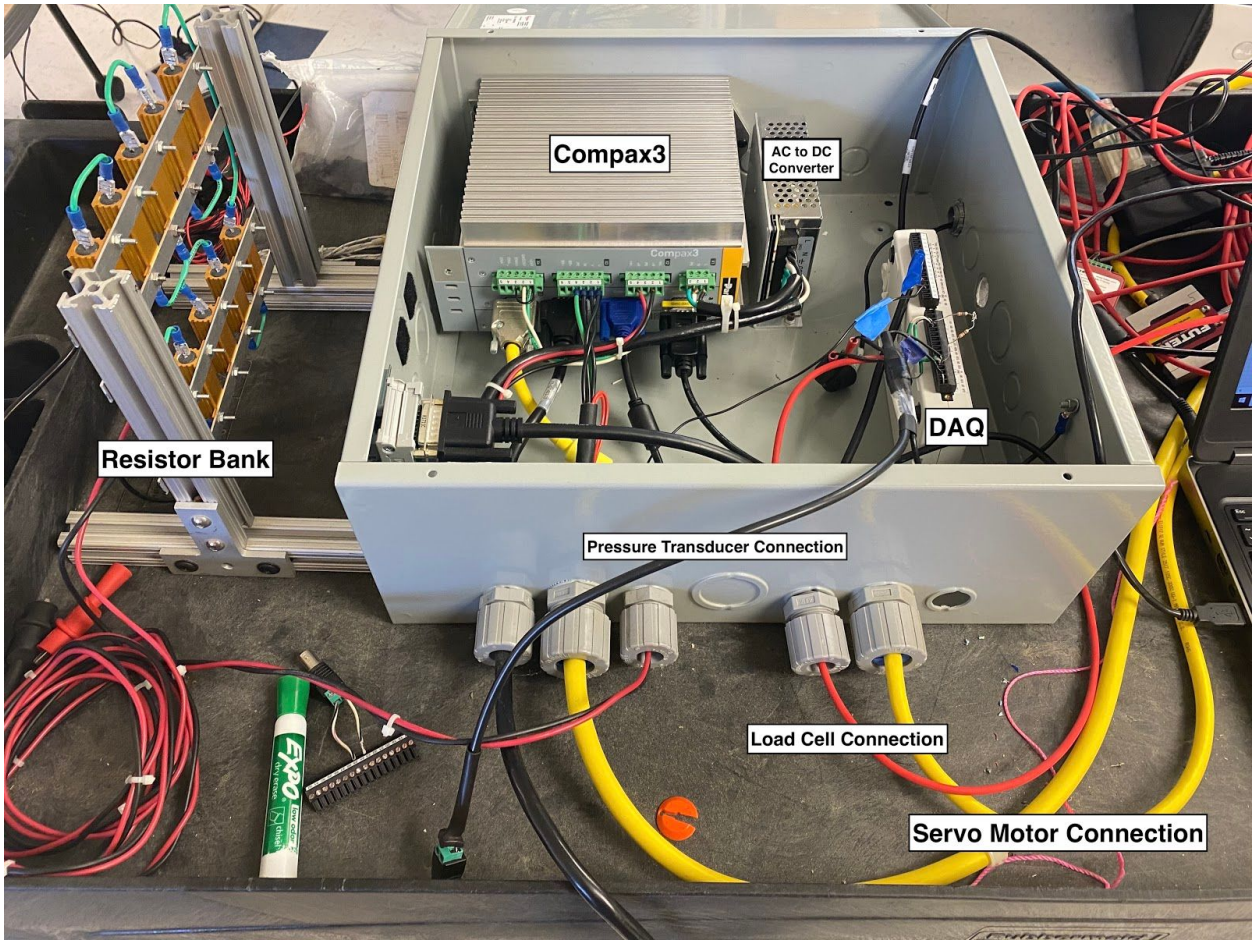

Figure 6.1 - Complete layout of the devices used to control the 1m HAWT.

To control the speed of the motor, the Compax3 is connected to the National Instruments 6211 DAQ as seen in Figure 6.2. With the connection to the DAQ, a maximum of 9.5 volts can be supplied to the motor which limits the motor from operating at maximum RPM. A more detailed wiring diagram of the DAQ can be seen in Figure 6.3. The two other major devices that are wired into the DAQ as shown in the figure are the load cell and the pressure sensor. The load cell is marked by the red wire which splits into three sub-wires all marked with a green casing. It is positioned at the base of the turbine tower and is used to measure the thrust of the turbine during different operating conditions. This device is important for obtaining thrust coefficient curves. The pressure sensor relays measurements that are taken from a pitot tube and run through a pressure transducer which outputs the pressure in torrs. The pitot tube is placed 3 meters in

front of the model wind turbine and a distance less than one meter from the turbine axis and is used to measure the speed of the incoming wind. Additionally, connection to the DAQ allows the measurements to control the speed of the motor. The last important wire component is the resistor bridge. This wiring technique is used to reduce the amount of noise in the data by having a central ground for the pressure sensor and the load cell.

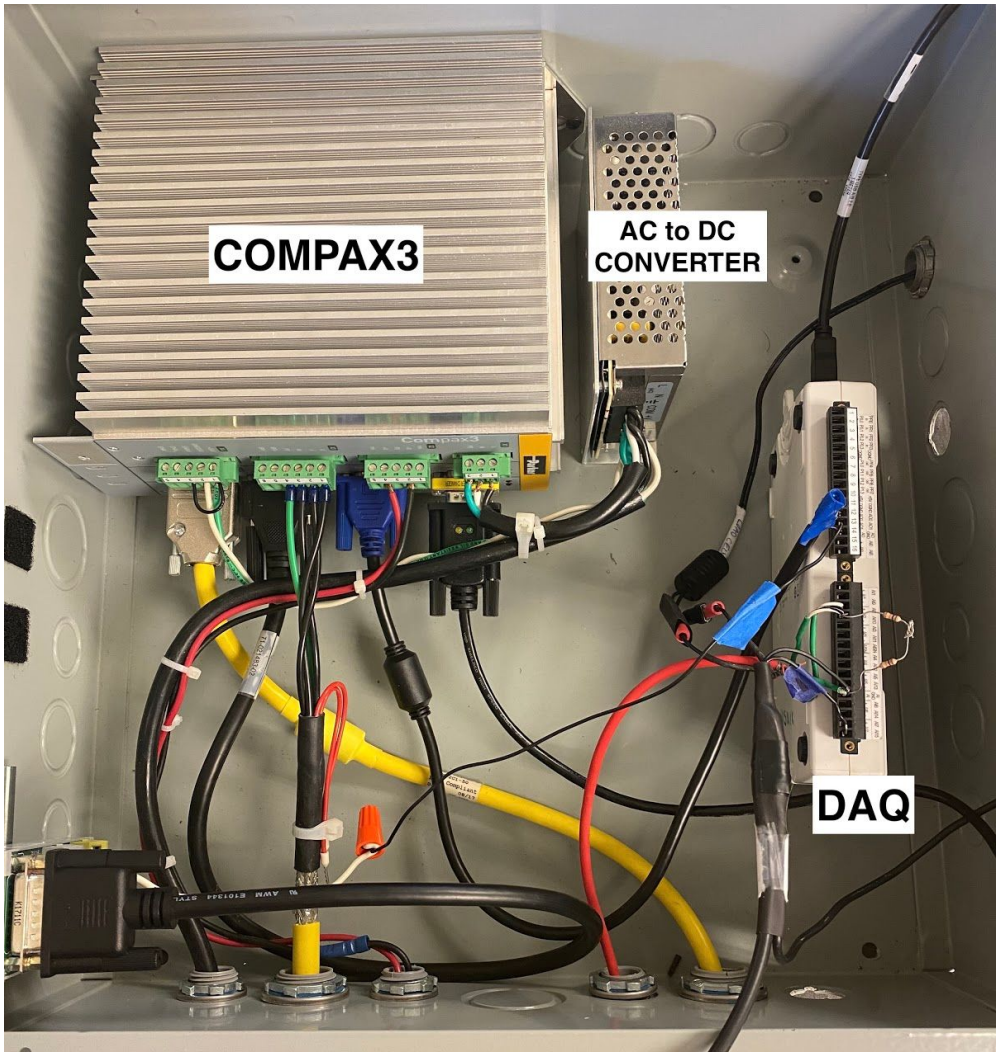

Figure 6.2 - Wire layout that connects the DAQ with the Compax3 used to power the 1m HAWT.

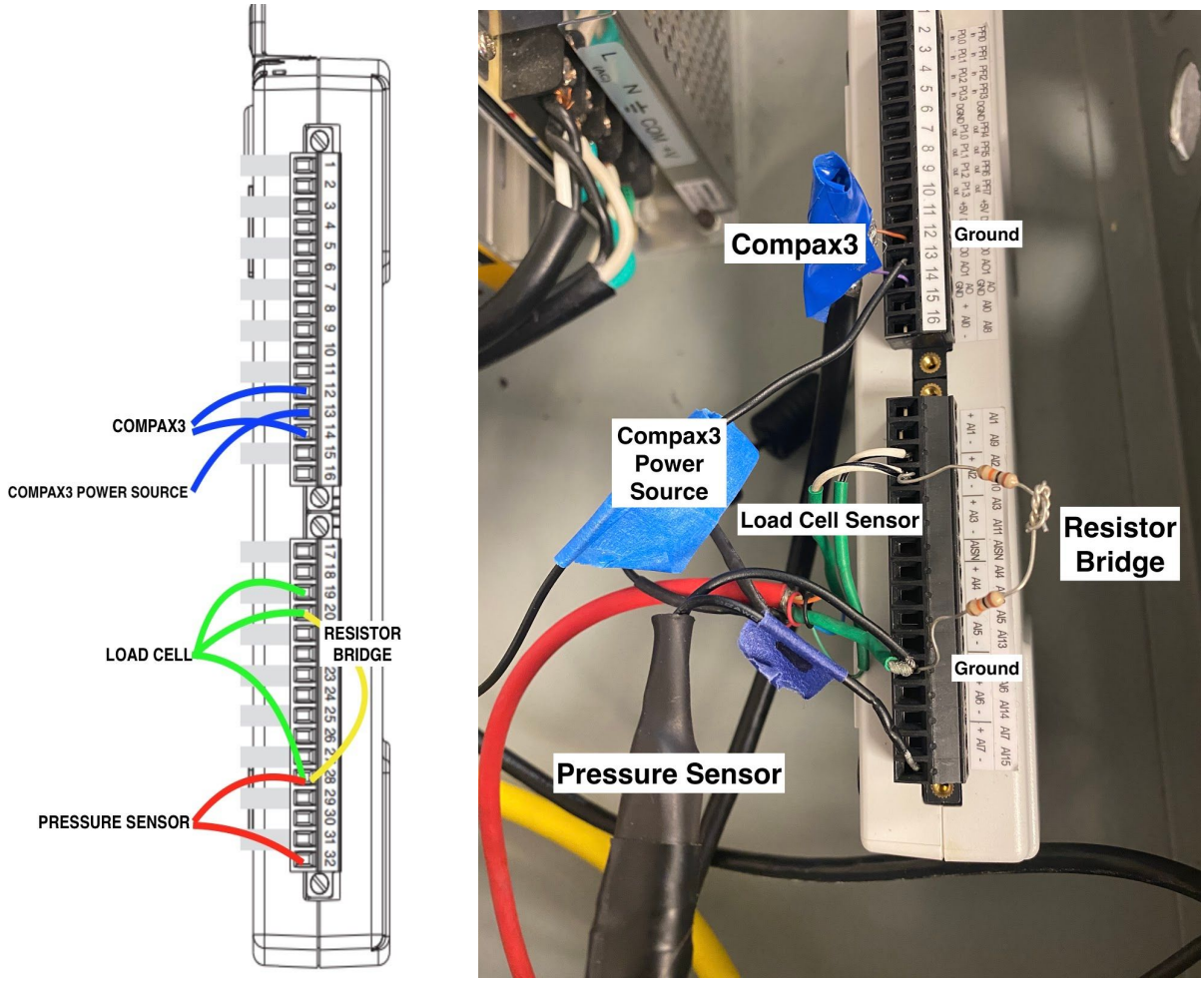

Figure 6.3 - Wiring connection diagram for the DAQ control system to control the 1m HAWT.

An overall block diagram for the electrical flow of the control system can be viewed in Figure 6.4. This block diagram, which was created by Jim Abare, maps out a detailed connection scheme as to how the Compax3 is integrated with the DAQ. Additionally, this diagram denotes the proper analog ports for each device as well as what each channel is on the Compax3.

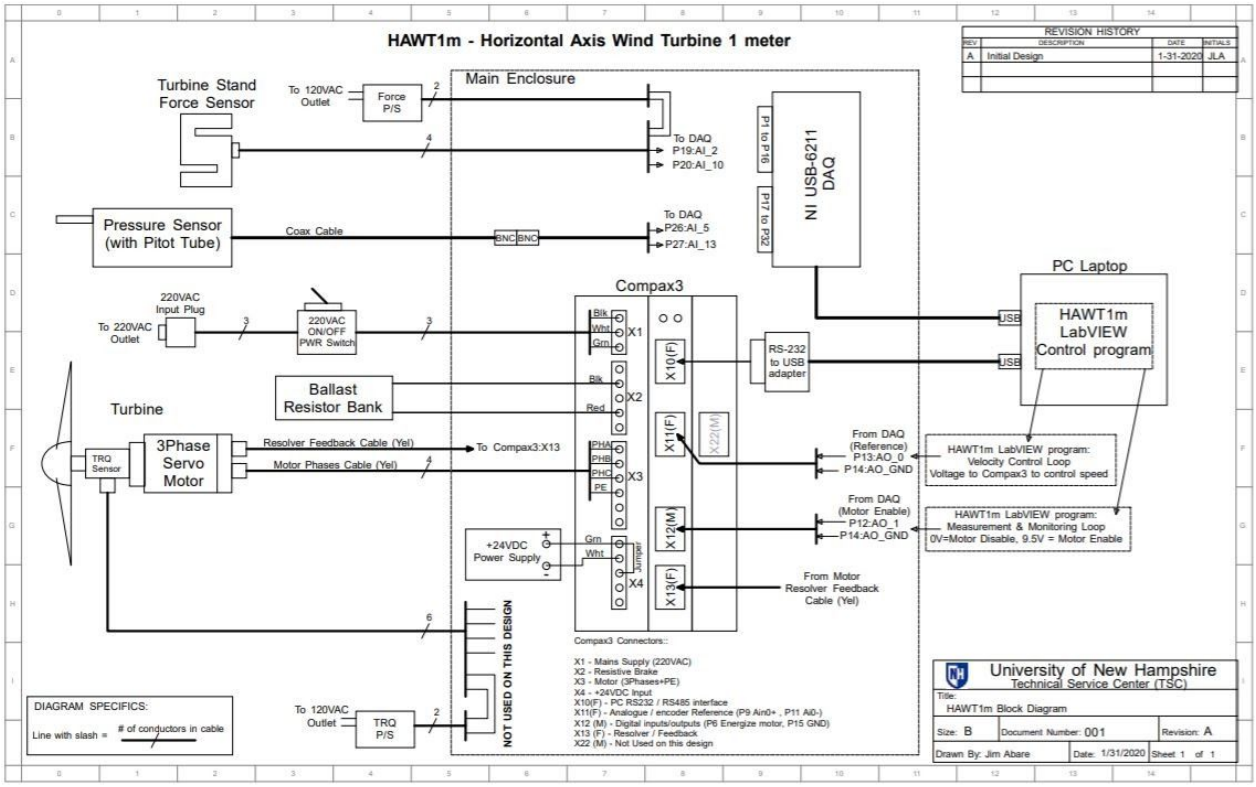

Figure 6.4 - Block diagram for the controls of the 1m HAWT [1].

In its current configuration, the DAQ is directly connected to the Compax3. This means that there is a low voltage source (the DAQ) wired to a high voltage source (the Compax3) which leaves the low voltage source vulnerable to the high voltage source. The DAQ's connected to the Compax3 also means that they share a common ground because there is a ground embedded into the Compax3. The common ground and the voltage danger lead to noisier data and a more dangerous setup. To combat this problem, below in Figure 6.5 is a proposed ground isolation circuit that should help both of those issues. This version of the circuit has not been tested yet but is believed to be a valuable and important addition to the controls of the 1m model HAWT.

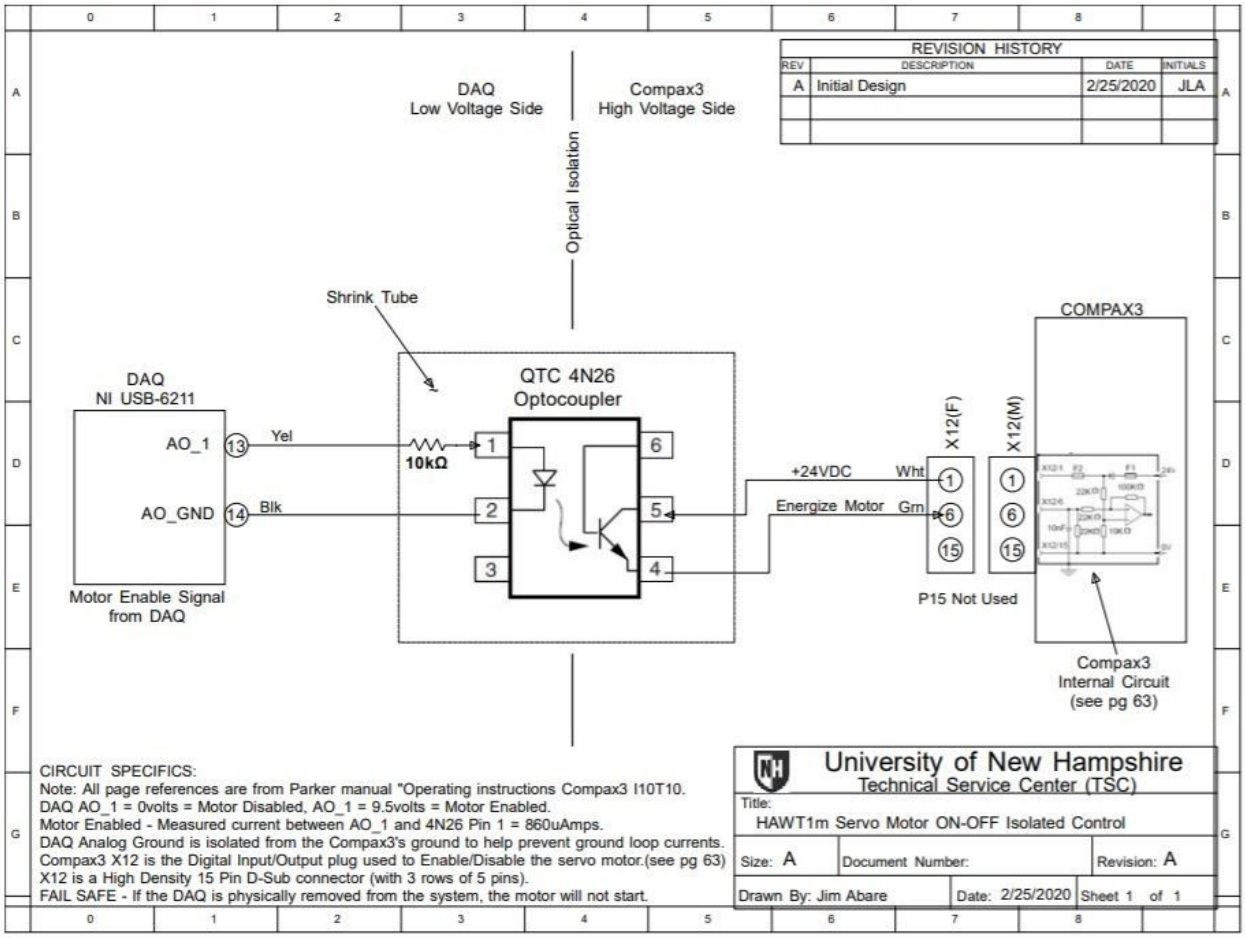

Figure 6.5 - Circuit diagram of proposed ground isolation [1].

7. Turbine Operation

7.1 Facility and Turbine Overview

Calibration and experimentation were all performed in the largest boundary layer wind tunnel in the world, the Flow Physics Facility (FPF), owned by and located at the University of New Hampshire. As stated in previous sections, the test section of the FPF is 72 meters long, 6 meters wide, and 2.7 meters tall. To account for the growth of the turbulent boundary layer, the ceiling height increases downstream. The gradual height change maintains a zero pressure gradient in the core of the test section [3]. Table 7.1 outlines the growth of the boundary layer on the four walls relative to two specified downstream locations for when the facility is operating at 7 m/s.

Table 7.1 - Boundary layer heights based on downstream location in the UNH FPF, [16].

Downstream Location	Boundary Layer Height	Test Section Velocity
4 (m)	.08 (m)	7 (m/s)
8 (m)	.14 (m)	7 (m/s)
16 (m)	.24 (m)	7 (m/s)
32 (m)	.43 (m)	7 (m/s)
66 (m)	.73 (m)	7 (m/s)

The FPF is powered by two 400 hp fans that are located at the exit of the facility. The fans draw the flow through the test section at a steady rate with a maximum free stream flow of 14 m/s (30 mph). The size of the test section allows for testing of the 1m scale wind turbine in both the free stream, toward the front of the test section, and under turbulent boundary layer conditions, near the back of the test section. The height of the boundary layer is not quite high enough to completely engulf the entire turbine at the back of the test section. However, with an obstruction (spires) in the front of the tunnel, a boundary layer of sufficient height can be created to test under designed conditions. A detailed rendering of the FPF is presented in Figure 7.1 below and outlines the major section previously mentioned.

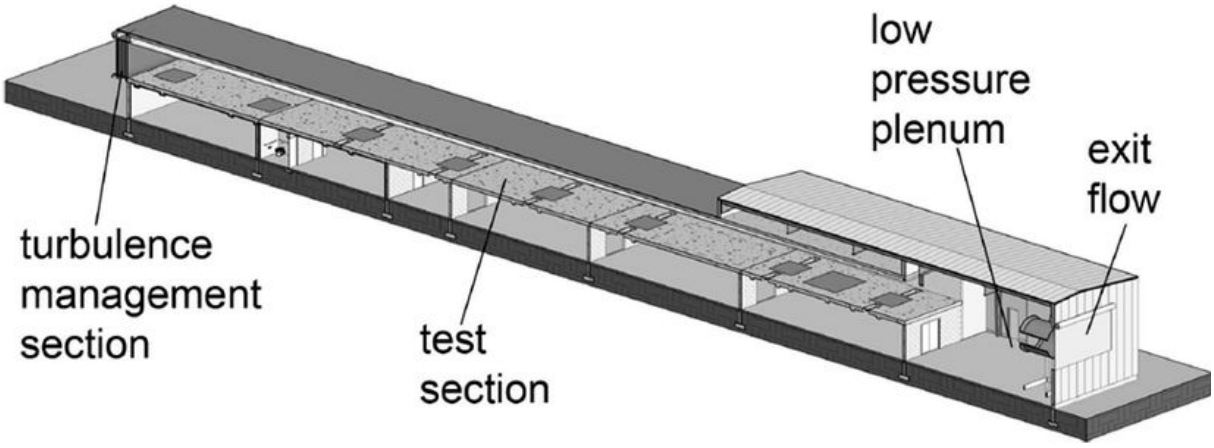

Figure 7.1 - Rendered view of the Flow Physics Facility (FPF) [3].

The model turbine was designed with the parameters of the FPF in mind. Modeled after the NREL 5MW reference turbine, it is scaled by a ratio of 1:126 [3]. The 1m HAWT is composed of five major components including the nacelle assembly, three custom designed blades, a unique pitch and hub control, a double stacked tower assembly, and a force balance for which the entire assembly sits on. A Solidworks rendering of the whole assembly details these main features in Figure 7.2 below.

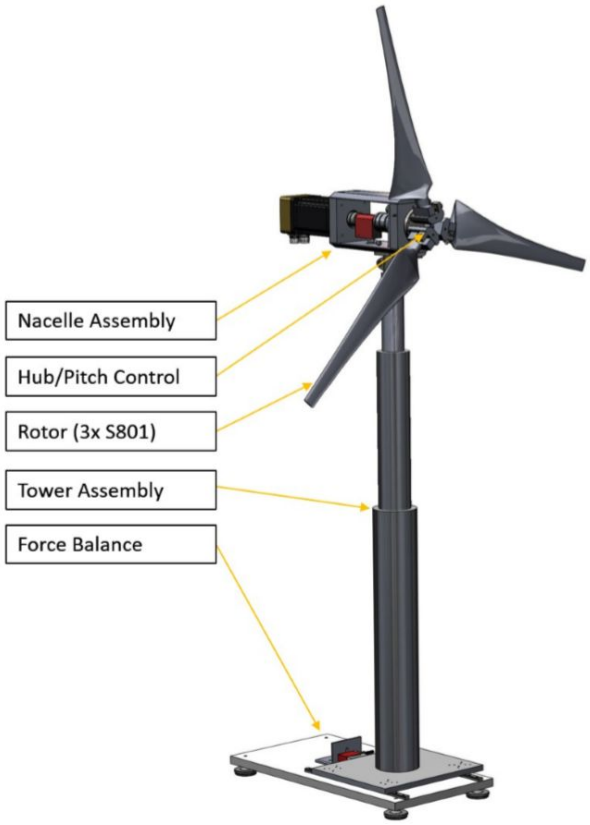

Figure 7.2 - Diagram of the 1m HAWT design [3].

The nacelle assembly consists of the servo motor which controls the speed of rotation of the blades when the turbine is just starting. A rotary torque transducer links in the midsection of the bearings and is used to measure the torque experienced by the turbine. Additionally, a machined bearing system connects to the hub that stabilizes the rotation of the turbine. It is through the torque transducer and the servo motor that power measurements can be observed. When fully assembled, the model wind turbine stands 1.35m tall at the turbine axis which is the exact midpoint of the wind tunnel.

A 1m diameter for the turbine cross section was chosen based on the cross section of the FPF. The large size of the test section allows the wind turbine to have a small enough blockage so that the coefficients of thrust and power are not affected. According to Sarlak, it was determined that a blockage exceeding 5% would begin to influence these coefficients [6]. When running, the turbine only blocks about 4.85% of the test section and therefore, power and thrust are not significantly affected.

7.2 Test Parameters

In order to analyze the performance of the 1m HAWT, two test scenarios will be used. The first will occur in the front of the wind tunnel using a uniform inflow and the second will occur in the back of the wind tunnel using an artificially thickened turbulent boundary layer. The procedure to test in both scenarios will be similar. First, everything will be set up and connected to power. In the first test, the turbine will be set up 8m from the inlet of the wind tunnel. There is a load cell placed at the bottom of the turbine on the force balance to measure the thrust felt by the tower from the wind. A pitot tube will be set up 5m from the inflow of the wind tunnel to measure the wind speed. This will then be used to help calculate the power available in the wind and the power converted from the wind by the turbine. The wind tunnel fans will be started at 600 RPM for the first iteration of the test and will increase at increments of 100RPM until 1000RPM. In each iteration, the program used to control the experiment starts the turbine running at a specific tip speed ratio based on input to the servo motors. This tip speed ratio will increase from 3.5 to 9 in 0.5 increments and will allow the program to find the maximum power, or where the turbine has the best performance at several different wind speeds. This test will be repeated three times with the turbine yawed at three different angles: 30^{o}, 0^{o}, and -30^{o}. Once the data is collected, it will be analyzed and the coefficient of power will be graphed against the actual tip speed ratio of the turbine. By analyzing the data with non-dimensional properties, the turbine can be compared to other turbines of similar size or to the NREL 5M reference turbine which it was modeled after. The data collected should be close to the data collected by Sam Cole when he first tested the turbine after it was built [3]. After the first test is complete, the second phase of testing will begin. During the second test, a barrier will be constructed and set up in the very front of the test section. The triangular spires will trip the inflow and create a taller

boundary layer which will be used to fully contain the turbine and simulate offshore wind conditions. The procedure of this test will be the same as the first test with the exception that it will occur in the back of the wind tunnel.

7.3 Labview Program

The program in LabView is the main control system for experimentation. In its original form, the program was set up as one giant loop that was completed at the same time. It collected data regardless of whether or not the data collection was needed (i.e. even when the wiring was being tested, data was collected), and to stop the program the stop button was hit which is essentially the same as forcing a shutdown on a laptop instead of going through the command sequence to turn it off. In order to make this program more effective and safer, it was completely re-written with the help of Jim Abare. It now has five loops which all complete different tasks. The first stage is the initializing stage and can be seen below in Figure 7.3.

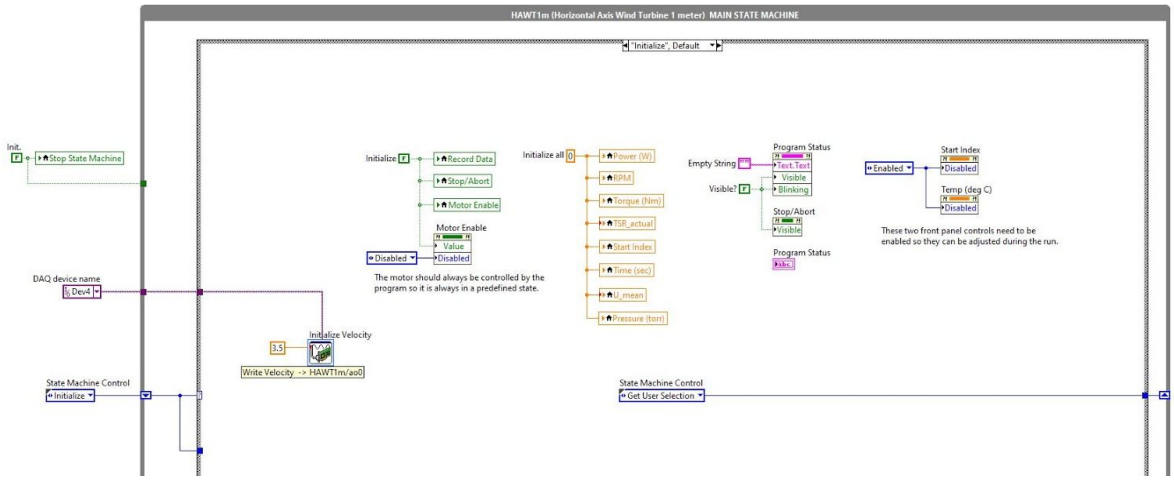

Figure 7.3 - LabView VI block diagram for: initialize testing.

In this stage of the loop, all the parameters are set to zero and the motor is enabled. On the outside of the loop are the things that do not need to be changed at every stage, like instrumentation. The top label, “stop state machine” is the safer method in which the program is stopped, the middle label, “DAQ device name” is the name of the DAQ being used to control the instrumentation, and the bottom label, “State Machine Control” controls which stage the machine is currently in. After the program is initialized, the next stage prompts the user as can be seen below in Figure 7.4.

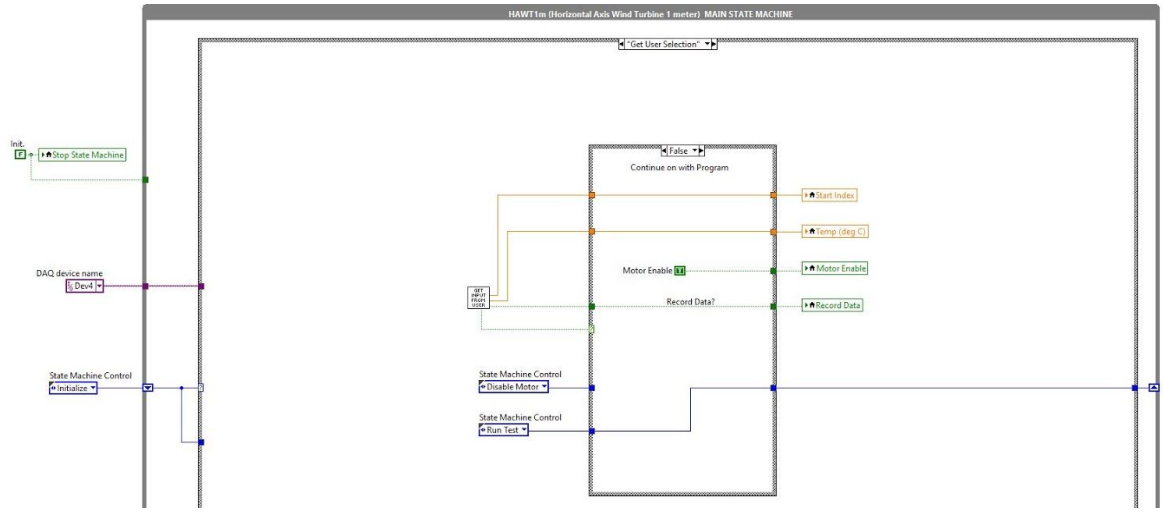

Figure 7.4 - LabView VI block diagram for: get user selection.

This stage of the loop prompts the user to input the current temperature in the tunnel and what the start index should be. It also asks the user if they want to collect data or if they want to run the experiment in a testing mode. Next is the most important stage of the program known as the run stage. It is shown below in Figure 7.5.

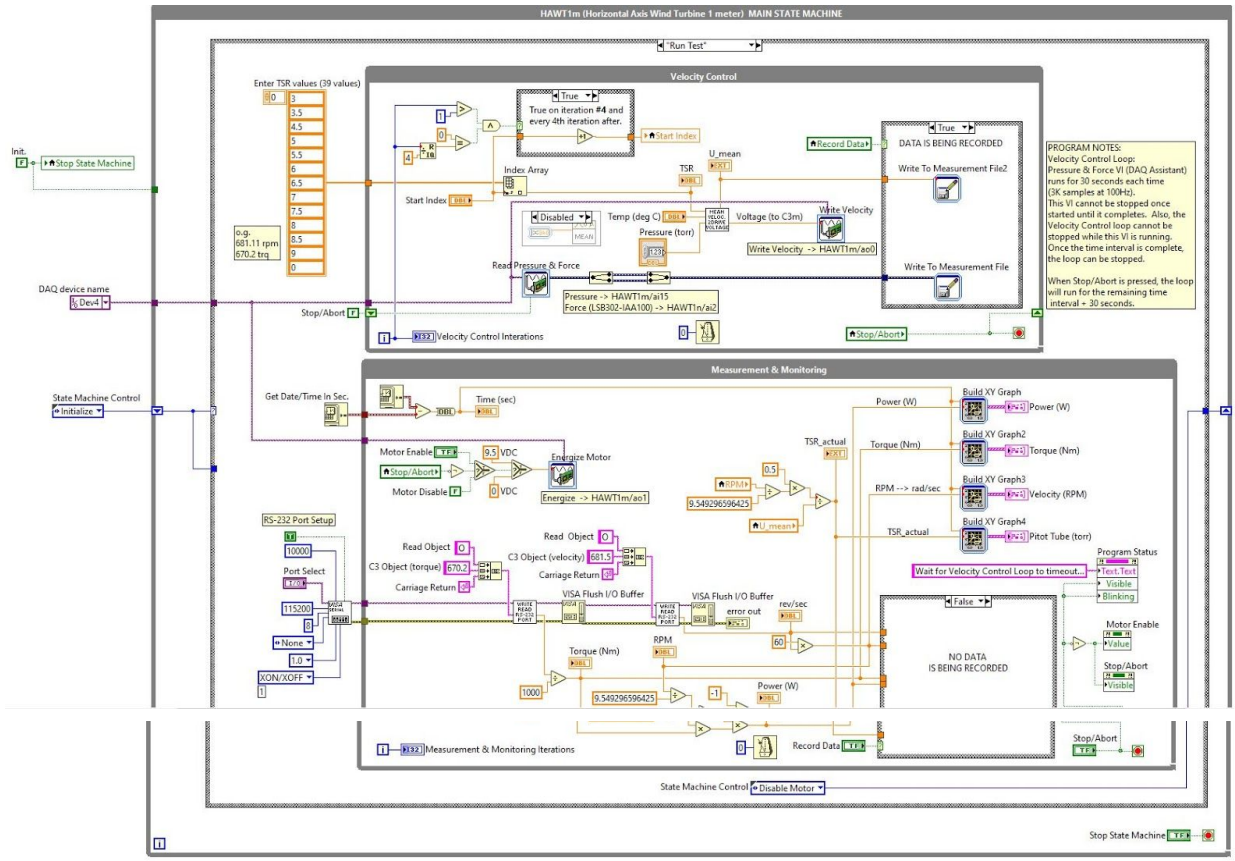

Figure 7.5 - LabView VI block diagram for: run stage of testing.

In the “Run” stage of testing, the most control and calculation heavy portion of the program is found. During this stage, the top loop is run through different indices which correspond to different tip speed ratios that are inputs to the system. The wind speed is also calculated here based on the pressure input into the front panel (Figure 7.8). Based on the TSR required and the wind speed input, the program writes a velocity which is sent to the motor in the bottom loop which is where the motor is enabled and told at what speed to spin. In the bottom loop is where the power output, torque output, actual TSR, pressure, and speed of the motor are all output to graphs and saved to excel files if the user asks to record the data in the previous stage. This stage is also where the stop control is initiated which stops the whole loop after waiting for the current period of data gathering times out. After the program stops, it goes to the next stage, “disable motor” which can be seen below in Figure 7.6.

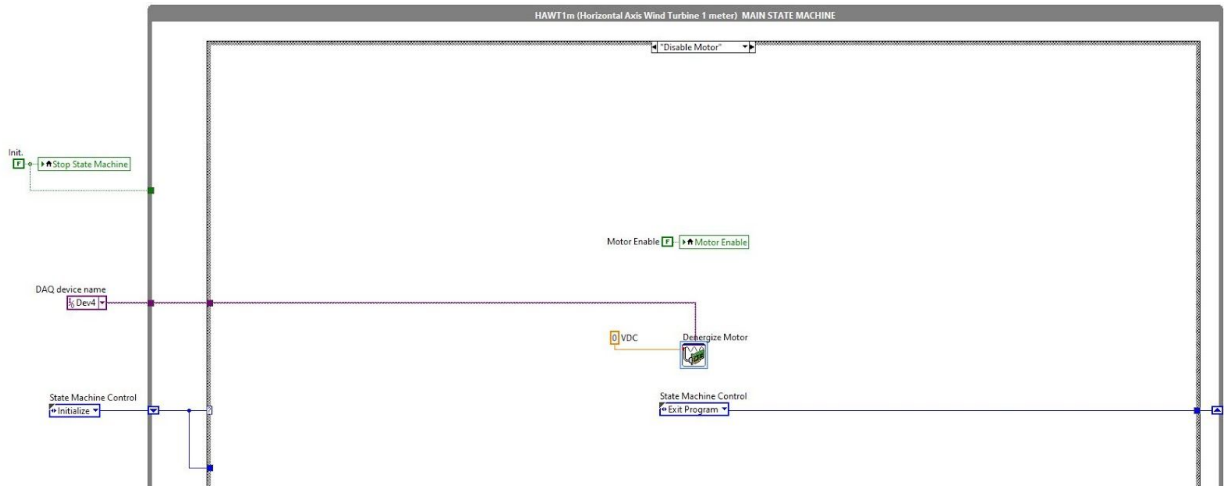

Figure 7.6 - LabView VI block diagram for: disable motor.

During this stage of the program, as the title says, the motor is disabled or shut down. After the motor is disabled, the program moves to the final stage as seen in Figure 7.7.

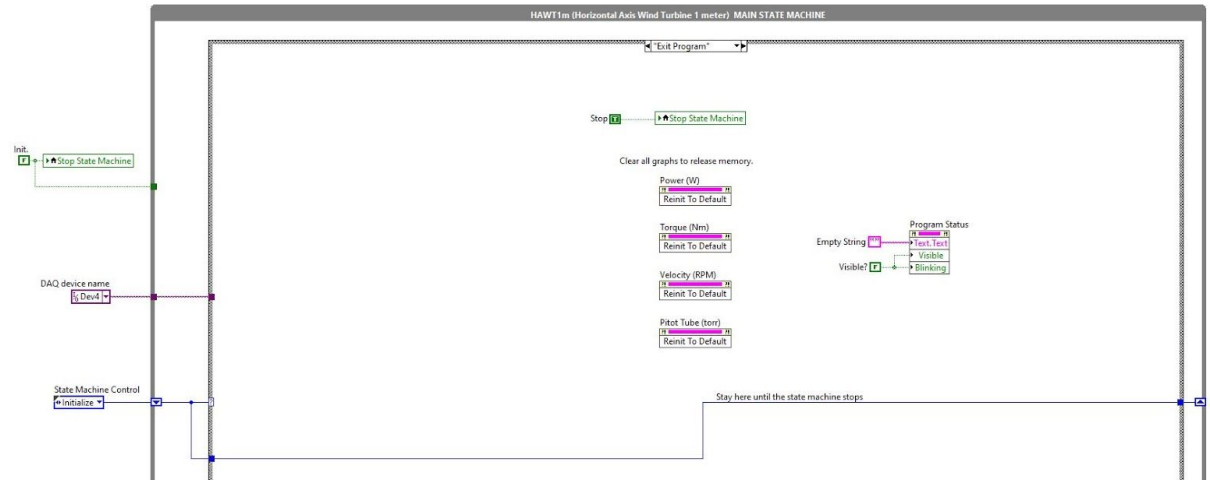

Figure 7.7 - LabView VI block diagram for: exit program.

In this stage of the program, the graphs are cleared and returned to their original states, the state machine is stopped and the program shuts down. This is the end of the test. Finally, Figure 7.8 below shows the front panel that the user interacts with to control the turbine.

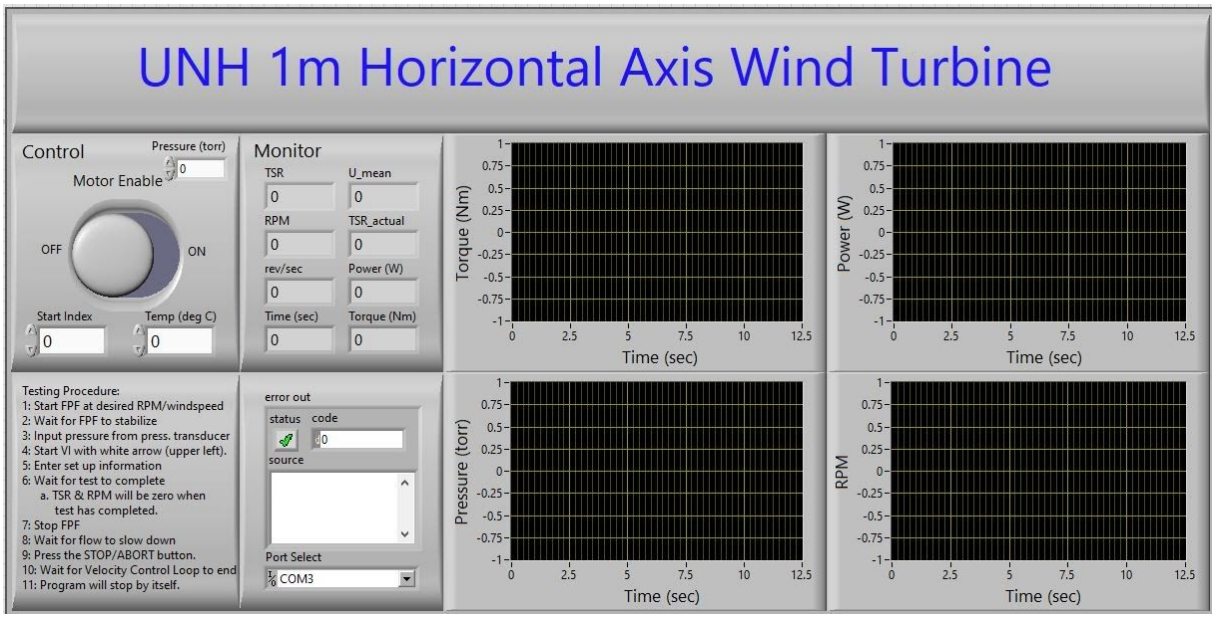

Figure 7.8 - Front panel of the HAWT control program.

Using this, the user will enter the pressure, start the program, be prompted to enter the start index and temperature and asked if they want to collect data or run in test mode. After that, the motor will start to run and the user will increase the start index to increase the TSR input which will then help to measure the performance of the turbine. After the user has finished testing, they can hit the stop button that appears in the top right corner of the front panel which will disable the motor and exit the program.

8. Performance Analysis

Most of the testing done using the 1m model HAWT is to determine the effects that different factors have on the performance of the wind turbine. These different factors include changing the yaw of the turbine, changing the type of inflow (uniform or turbulent boundary layer), changing the pitch of the blades, etc. In order to compare how the different factors affect the performance and subsequently extrapolate the data to real world situations and turbines, the data collected has to be analyzed in a way that allows for a non-dimensional comparison. The most typical method of doing so in industry is by the creation of coefficient of power (C_p) vs tip speed ratio (λ) and coefficient of thrust (C_T) vs tip speed ratio (λ) graphs. In this case, the data collected is gathered by LabView and then processed using a MATLAB program. The power output of the turbine, actual tip speed ratio of the rotor, pressure drop across a pitot tube, thrust on the tower, torque of the motor, RPM of the motor, and temperature of the tunnel are output from the LabView program and gathered into excel data sheets. This data can then be loaded into MATLAB for analysis. As previously stated, the best way to non-dimensionally view performance results is by creating a C_p vs λ graph. In order to do so, the data is run through a for loop within the MATLAB analysis to determine the air density, the wind speed, the theoretical power output, and the coefficient of power. The following equations are used to determine those outputs:

$$\rho = P/RT \tag{8.1}$$

Where ρ is air density using a measured pressure, P, a gas constant, R, of 287.05 J/kgK, and a temperature, T, based on the temperature in the tunnel. Next, the wind speed can be calculated using the air density found and the following equation:

$$U_\infty = \sqrt{\frac{2(p*133.32)}{\rho}} \tag{8.2}$$

In this equation, U_∞ is the average wind speed of the tunnel where the wind turbine is set up, p is the differential pressure readout from the pressure transducer which is multiplied by 133.32 to convert from torrs to Pa, and ρ is the air density calculated in the previous equation. After finding the average wind speed of the tunnel, the available power in the wind could be found using the following equation:

$$P_{available} = \tfrac{1}{2}\rho A_{rotor} U_\infty^3 \tag{8.3}$$

In this equation, P is the theoretical power output, ϱ is the air density found in equation 8.1, A_{rotor} is the area of the rotor intercepting the wind, and U_{∞} is the average wind speed found in equation 8.2. Based on this information calculated from the wind tunnel current conditions, and the information given by from the LabView output, the coefficient of power can be found.

$$C_p = \frac{P_{actual}}{P_{available}} \tag{8.4}$$

Tip speed ratio, λ, is already an output of the LabView program, and with the coefficient of power calculated, the graph to non-dimensionally determine turbine performance can be created. This graph will be the main mode of comparison for the effects of yaw, blade pitch, and inflow shape.

In order to fully analyze the performance of the turbine, the theoretical performance must first be found. This analysis was completed using a program called Qblade. Qblade uses blade element momentum theory or BEM to analyze different airfoil profiles and blade shapes at specific Reynolds numbers. From Sam Cole's thesis, it is known that the airfoil used for the blades is a NREL S801. For ease of manufacturing, the same airfoil was used throughout the entire blade length. The NREL S801 profile is shown below in Figure 8.1 as it appears in the Qblade program from data points provided by NREL [9].

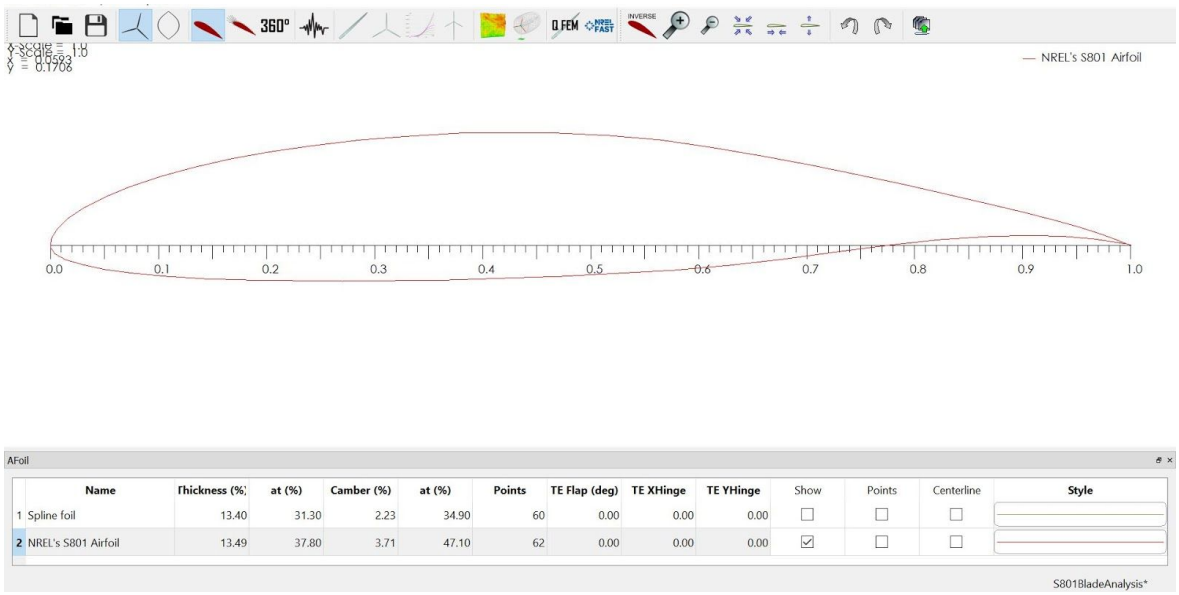

Figure 8.1 - Profile view of the blade element design for the 1m HAWT.

The next step in the blade analysis is to find the polars of the airfoil profile which were found using a N_{crit} value of 5 and a Reynolds number of 149,000. Both of these values were based on the findings of the blade design selection process outlined in Sam Cole's thesis [3].

From there, the polar created could be extrapolated to 360°. The graph below pictured in Figure 8.2 is one of the results of that extrapolation.

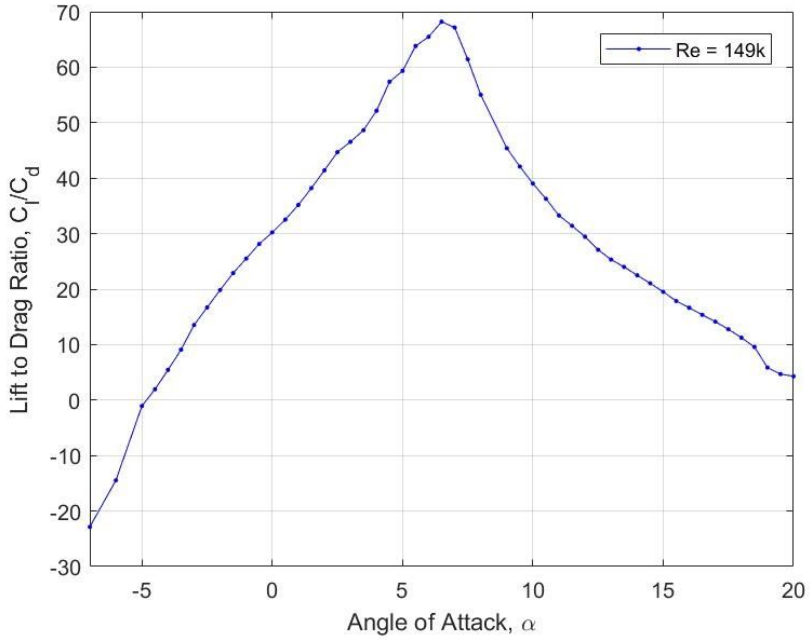

Figure 8.2 - Ratio of the lift coefficient to the drag coefficient vs the angle of attack.

The above graph shows the lift drag performance of the S801 airfoil at different angles of attack. The most important and relevant part of the graph is the middle section between angles of attack of -10° to 20°. This shows that there is a fairly linear performance curve between 0° and 10° which is close to the design angle of attack. It also has a relatively high peak in this location showing that there is more lift than drag meaning that the airfoil would perform best at the design angle of attack.

To create the theoretical non-dimensional performance curve, C_p vs. λ, a full blade had to be created. The figure below shows the shape of the blade created. The blade is 0.425m long, as the diameter of the rotor is 1m including the hub. The hub has a radius of 0.075m which is where the root of the blade begins. This blade is based on the actual blade of the 1m model HAWT which means that the chord is 1.35x the optimal chord. However, the optimal twist was retained and was found using Qblade's option to optimize the blade twist based on the Betz limit.

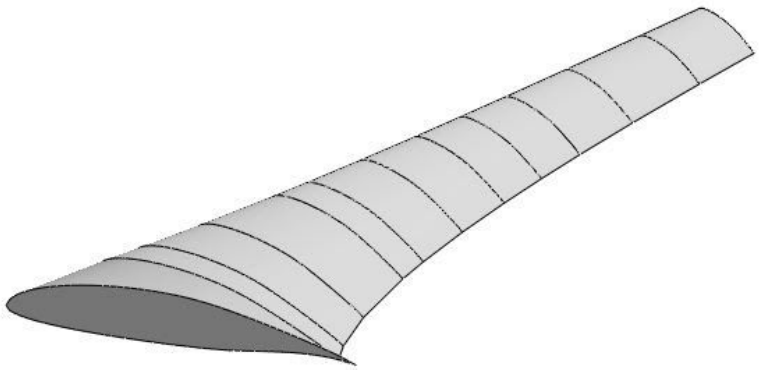

Figure 8.3 - Qblade model of the blade used for the 1m HAWT.

Using the model above, the next step in the analysis was to analyze the performance using the rotor BEM simulation. When running the simulation and defining the parameters, the average wind speed was chosen to be 10m/s and the simulation includes effects of Prandtl tip loss and Reynolds drag correction. The simulation was run with tip speed ratios ranging from 1 to 10 in increments of 0.1. The curve shown below in Figure 8.4 is the result of the analysis. As can be seen in the figure, the peak performance at 10m/s occurs at a tip speed ratio of approximately 6.1. This result matches what was found in a previous study.

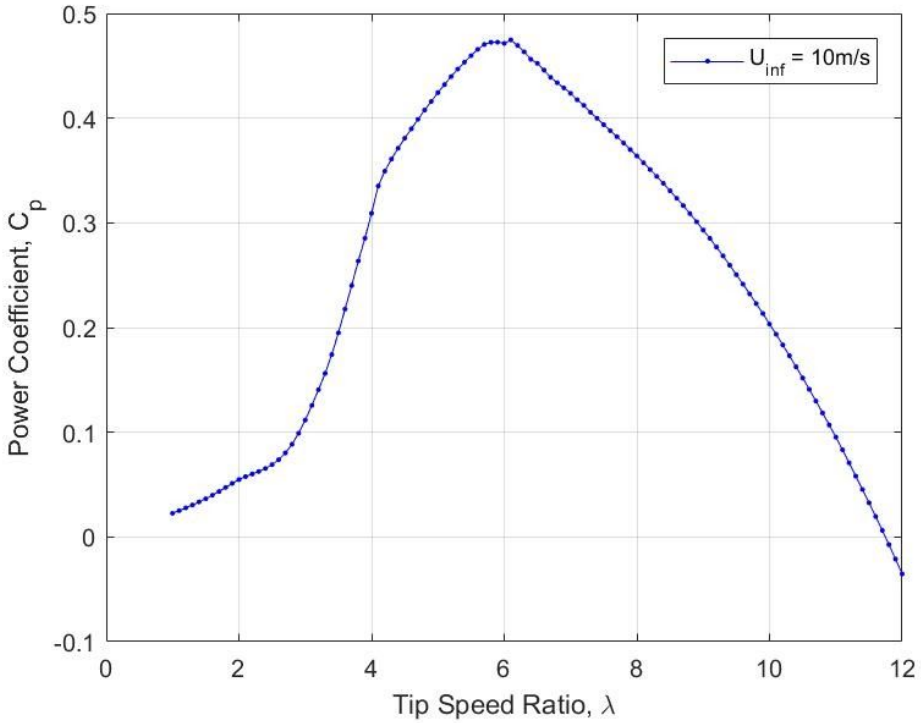

Figure 8.4 - Theoretical power coefficient as a function of tip speed ratio for the specified 1m HAWT blade design. The power coefficient peaks at about 0.47 with a tip speed ratio around 6.

Based on the coefficient of power versus tip speed ratio curve above, a brief qualitative analysis can be done to compare these results to the actual performance results gathered in previous studies. Figure 8.5 shows the non-dimensional power curve from previous experimentation using the 1m model HAWT in different wind speeds.

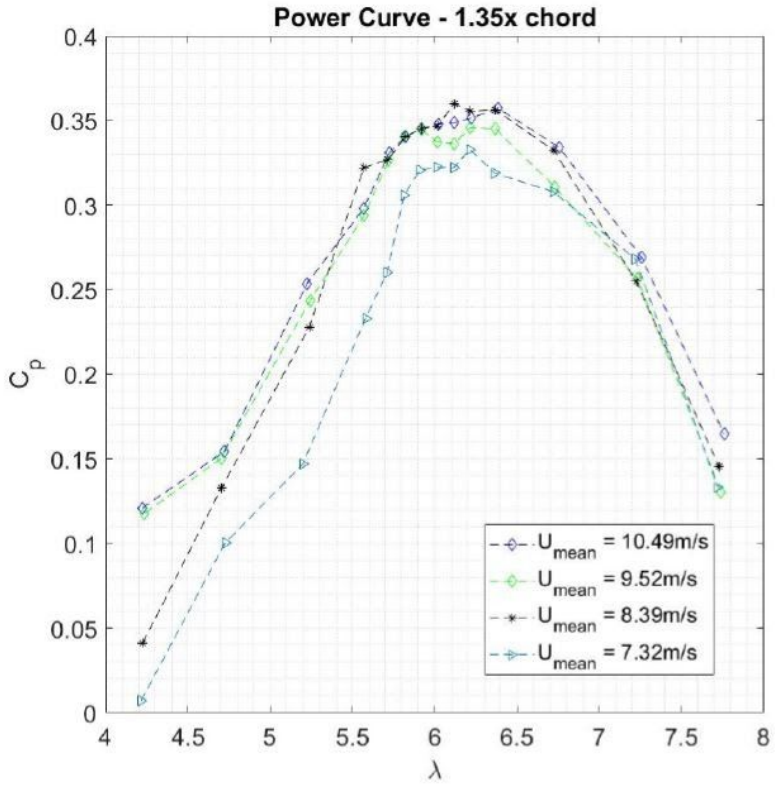

Figure 8.5 - Non-dimensional power curve from previous experimentation [3].

In this graph, it can be seen that when the mean wind speed was 9.5m/s the coefficient of power peaked around 0.35 with a tip speed ratio of about 6.2. It can also be seen that when the mean wind speed was 10.5m/s the coefficient of power peaked around 0.36 when the tip speed ratio was 6.4. The Qblade analysis was performed assuming an average wind speed of 10m/s which is halfway in between those two. Assuming that there is a linear correlation between the speed, peak coefficient of power, and tip speed ratio, this would lead to a peak coefficient of power of about 0.355 at a tip speed ratio of 6.3 when the average wind speed was 10m/s. When those results are compared to the theoretical results from the Qblade analysis it can be seen that while the tip speed ratio at the peak coefficient of power was only slightly higher than that of the theoretical, the coefficient of power was significantly lower than what was found in the theoretical analysis. This could be because the efficiency of the motor and the torque transducer was not taken into account during the Qblade analysis, or because the wind fluctuates more in reality than in the theoretical simulation.

9. Spire Analysis

In order to test the turbine in offshore wind conditions, the turbine needs to be fully ensconced within a simulated atmospheric boundary layer. The nature of the FPF is such that it naturally creates a boundary layer as the inflow moves down the tunnel. However, because the model HAWT used is so large, a larger boundary layer needs to be created to more accurately simulate offshore wind conditions. To do this, the inflow needs to be tripped using spires to create a larger boundary layer. Figure 9.1 below shows how the boundary layer is created through the use of spires. In this case, the thickness needs to be taller than the height of the wind turbine in its shorter form. The tallest point of the turbine in its shorter form is 1.21m tall. Based on this, a boundary layer thickness of 2m was chosen as the goal.

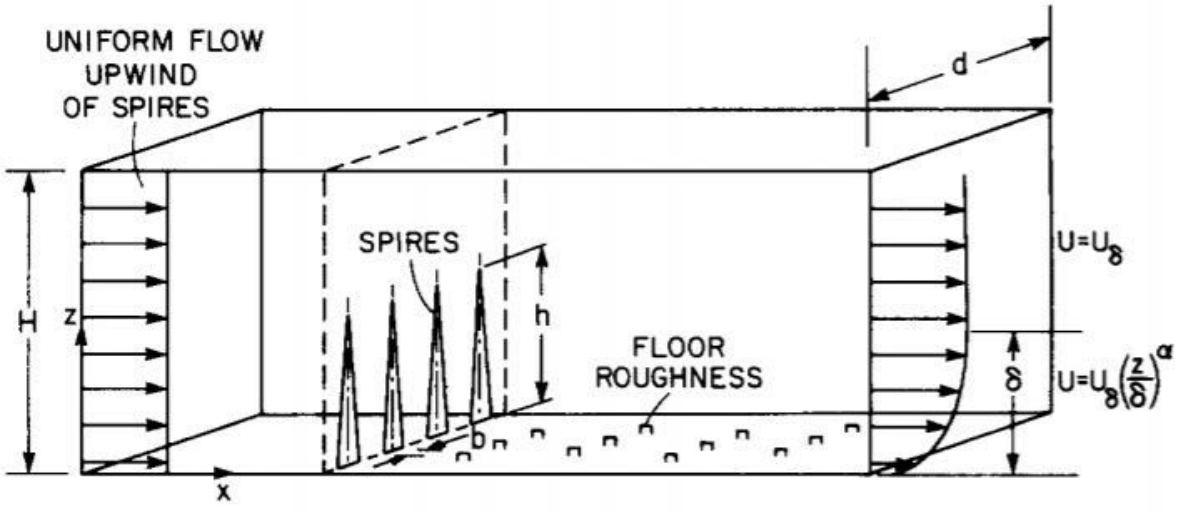

Figure 9.1 - Diagram of wind tunnel with spires and floor roughness elements included [8].

Using a previous study done on the creation of spires to simulate a turbulent boundary layer, the following process was used to calculate the necessary geometry for the desired boundary layer [8]. To achieve a boundary layer, $\delta = 2$ meters high, with a power law exponent of $\alpha = 1/7$; the height of the spires needed would be defined by equation 9.1.

$$h = 1.39\,\delta\,/(1 + \alpha/2) \tag{9.1}$$

The base is then found using the base to height ratio equation below,

$$b/h = 0.5[\,\psi(H/\delta)/(1 + \psi)](1 + \alpha/2) \tag{9.2}$$

where equation 9.3 and equation 9.4 describe the parameters ψ and β in equation 9.2.

$$\psi = \beta\{[2/(1 + 2\alpha)] + \beta - [1.13\alpha/(1 + \alpha)(1 + \alpha/2)]\}/(1 - \beta)^2 \quad (9.3)$$

$$\beta = (\delta /H)\, \alpha/(1 + \alpha) \quad (9.4)$$

Next, to determine the skin friction coefficient the following equation was used,

$$C_f = 0.136[\alpha/(1 + \alpha)]^2 \quad (9.5)$$

Based on this equation and the values of δ, C_f, and the distance between the floor roughness elements, D, the ratio between the roughness element height, k, and the boundary layer thickness, δ, could be found using the following equation,

$$k/\delta = exp\{(\tfrac{2}{3})ln(\tfrac{D}{8}) - 0.1161[(\tfrac{2}{C_f}) + 2.05]^{1/2}\} \quad (9.6)$$

(In the above equation, the distance between the floor roughness elements was chosen to be 5m) Based on the thickness needed and the alpha chosen, the following results were found:

Table 9.1 - Results of spire analysis.

h	2.6m
b	0.09m
C_f	0.0021
k	0.041m

These equations assume that a boundary layer of the desired thickness is fully formed 6h from the spires. From previous inflow tests conducted in the FPF, it is known that a fully formed uniform inflow can be found 6m from the test section entrance. If the spires are set up here, then the wind turbine should be set up at least 15.6m from the spires or 22m from the entrance of the test section. However, based on previous studies done in the FPF with spires, in experimentation, the turbine may need to be set up significantly farther back than 22m in order to achieve the desired boundary layer. In the figure below, Figure 9.2, a detailed diagram of an individual spire can be seen. The splitter plate pictured in the back of the spire is used to support the spire and ensure that it remains in place during testing.

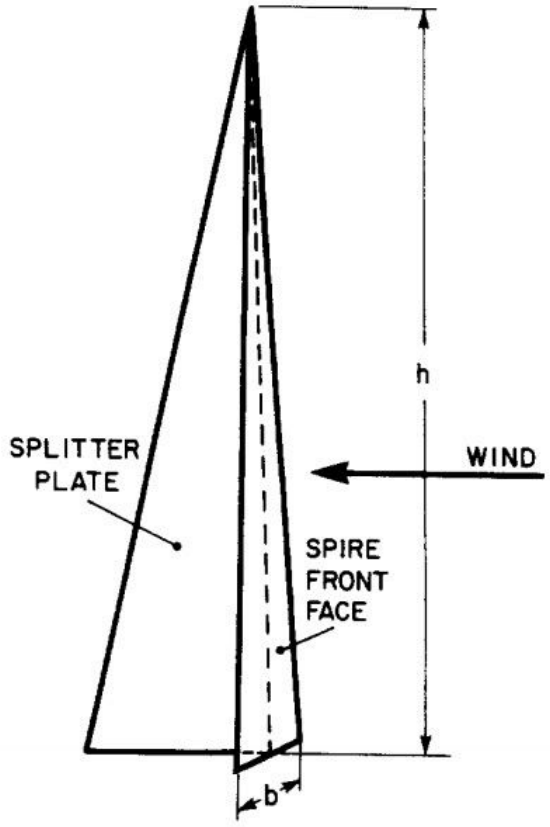

Figure 9.2 - Diagram of a triangle spire with a splitter plate [8].

To see if there is interference with the boundary layer formed by the spires on the lower floor and the boundary layer formed on the three other walls in the wind tunnel, basic calculations were performed using equations 9.7 and 9.8. Shortly after the inlet of the turbine, the flow reaches a turbulent state. The boundary layer for turbulent flow can be described as,

$$\delta = \frac{0.382\ x}{\sqrt[5]{Re}} \tag{9.7}$$

where x is the length of surface to where the model wind turbine is positioned and Re is the Reynolds number for the particular test wind speed. The Reynolds number can be determined using equation 9.8,

$$Re = \frac{U_\infty x}{\nu} \tag{9.8}$$

where U_∞ is the speed of the wind flowing through the tunnel, x is the length of the surface, and ν is the kinematic viscosity of air which.

Through this estimation, with a wind speed of about 10m/s the maximum boundary layer formed on the three walls 22m downstream was 0.44 m from the surface. Therefore, given that the height of the boundary layer formed by the spires is 2 meters and the height of the wind tunnel is 2.7 meters, there is no interference between the floor and ceiling boundary layers at this distance downstream. The turbine will be positioned in the middle of the test section meaning and given that the turbine is only 1m wide and the test section is 6m wide, there is no interference from the boundary layers developed on the side walls either.

10. Summary

Validating wind turbine performance is a growing and necessary field. Wind turbines are increasingly being used across both the country and the world as a source of renewable energy, and are being deployed both as single turbines and in arrays known as wind farms. The configuration of these wind farms has also become a more important topic as performance validation research is conducted on the effects of turbine wakes on the performance of other turbines. Wake steering is a method in which the turbines of a wind farm are yawed out of the wind (at an optimal angle) to maximize the power of the turbines in the farm, and minimize the effects of the turbulent wakes on other turbines in the wind farm. By studying the performance of wind turbines in yawed conditions and measuring their wakes, the benefits of wake steering to optimize a wind farm as a whole can be validated. In order to contribute to the research that is being done, the UNH research team used a 1m model HAWT in the FPF to study wind turbine performance. The UNH FPF is the longest boundary layer wind tunnel in the world, and because it is a wind tunnel, the inflow is more easily controlled than in a full-scale field test. Both of these qualities are important in conducting these validation experiments. Before testing, however, the 1m model HAWT had to be rewired due to unexpected instrumentation loss. The goal of this thesis was to provide documentation on what the research team worked on in addition to background information on the topic, theoretical analysis, and future experimentation hopes.

Documentation of the progress made was the most important goal of the thesis. The team wanted to ensure that future researchers using the same equipment would be able to completely reconstruct the turbine's wiring on their own. In this thesis, that meant that extensive wiring diagrams were included as well as descriptions of the various instruments used and how they all contributed to the controls of the system. The control program written in LabView was also discussed and documented for the same reasoning: enabling future users to have more confidence in the workings of the control systems. Finally, the analysis method was also documented in the background section and the performance section to provide more information about wind turbines and how to complete a performance analysis.

The theoretical analysis completed by the team used Qblade to analyze the performance of the turbine under ideal conditions. For the Qblade analysis, the NREL S801 airfoil was used and the blade was created to have the optimum twist using the Betz limit, but 1.35x the optimum chord using the lift to drag ratio. From that the coefficient of power versus tip speed ratio was created for a wind speed of 10m/s. At this speed, the peak power coefficient was 0.47 and occurred at a tip speed ratio of 6.1. This was compared to the actual results from previous experimentation and while the tip speed ratio where peak performance occurred was similar, the peak coefficient of power was significantly lower with values of 6.3 and 0.35 respectively.

Finally, the necessary spire height for simulated offshore conditions was calculated. Based on the parameters chosen, the necessary spire height to create a turbulent boundary layer of the appropriate thickness was found to be 2.6m tall with base widths of 0.09m. The height of the roughness elements was found to be 0.041m. Using spires and roughness elements of these dimensions should create a boundary layer of the appropriate thickness at a distance 16m downstream of the spires. However, testing of the flow conditions at this location should be done to confirm that the flow is indeed the correct shape. Based on the information given in this report, future users of the equipment should be able to conduct experiments with more confidence and further aid wind turbines, and consequently wind farm design.

11. References

[1] Abare, J. (2020). Electrical and LabView knowledge [In person]. University of New Hampshire.

[2] "China Starts Building First 10-GW Mega Wind Farm." *Reuters*, Thomson Reuters, 8 Aug. 2009,www.reuters.com/article/us-china-wind-power/china-starts-building-first-10-gw-mega-wind-farm-idUSTRE5771IP20090808.

[3] Cole, S. (2018). *Design and performance of a 1 meter horizontal axis wind turbine model* (Graduate). University of New Hampshire.

[4] Fleming, P. *et al* 2016 *J. Phys.: Conf. Ser.* 753 052003 https://iopscience.iop.org/article/10.1088/1742-6596/753/5/052003/pdf

[5] Fleming, Paul, Annoni, Jennifer, Shah, Jigar J., Wang, Linpeng, Ananthan, Shreyas, Zhang, Zhijun, Hutchings, Kyle, Wang, Peng, Chen, Weiguo, & Chen, Lin. *Field Test of Wake Steering at an Offshore Wind Farm*. United States. doi:10.5194/wes-2017-4. https://www.nrel.gov/docs/fy17osti/67623.pdf

[6] H. Sarlak, J. Sorenson, T. Nishino, L. Martinez-Tossas, and C. Meneveau. Assessment of blockage effects on the wake characteristics and power of wind turbines. Renewable Energy, 2015

[7] "How Wind Energy Works." *Union of Concerned Scientists*, 14 July 2008, www.ucsusa.org/resources/how-wind-energy-works.

[8] Irwin, H. (1981). The design of spires for wind simulation. *Journal of Wind Engineering & Industrial Aerodynamics, 7*(3), 361–366. https://doi.org/10.1016/0167-6105(81)90058-1

[9] Jonkman, B. (2014). *S801 Airfoil Shape*. NREL - NWTC Information Portal. Retrieved 24 April 2020, from https://wind.nrel.gov/airfoils/Shapes/S801_Shape.html.

[10] Parker Hannifin Corporation. (2010). *Operating Instructions Compax3 T30* [Ebook]. Retrieved 24 April 2020, from http://www.logic-control.com/datasheets/28/Compumotor/Compax3/T30%20User%20Guide.pdf

[11] Runyon, Jennifer. "History of Wind Turbines." *Renewable Energy World*, 9 Sept. 2019, www.renewableenergyworld.com/2014/11/21/history-of-wind-turbines/#gref.

[12] Song, P. (2017). Simulation of Atmospheric Boundary Layer in an Open-Loop Wind Tunnel Using Spire-Roughness-Element Technique. https://pdfs.semanticscholar.org/beb8/89fc30aed7b2ce9d7961dd9cbd1111a8b94f.pdf?_ga=2.151590201.1653337999.1586876001-369242932.1586876001

[13] *SWiFT Facility & Testing*. Sandia National Laboratories: Energy. (2015). Retrieved 24 April 2020, from https://energy.sandia.gov/programs/renewable-energy/wind-power/wind_plant_opt/.

[14] Taylor-Power, G. (2018). *Experimental investigation of the turbulent wakes generate by wind turbine models in a large boundary layer wind tunnel* (Graduate). University of New Hampshire.

[15] Uncertainty: Coleman, Hugh W., and W. Glenn. Steele. *Experimentation, Validation, and Uncertainty Analysis for Engineers*. 3rd ed., Wiley, 2018.

[16] Vincenti, P. and Klewicki, J. and Morrill-Winter, C. and White, C. and Wosnik, M. Streamwise velocity statistics in turbulent boundary layers that spatially develop to high Reynolds number. Experiments in Fluids, 54, 12 2013.

[17] *Wind explained: Electricity generation from wind*. eia: U.S. Energy Information Administration. (2020). Retrieved 24 April 2020, from https://www.eia.gov/energyexplained/wind/electricity-generation-from-wind.php.